Univerzita Karlova v Praze
Matematicko-fyzikální fakulta

DIPLOMOVÁ PRÁCE

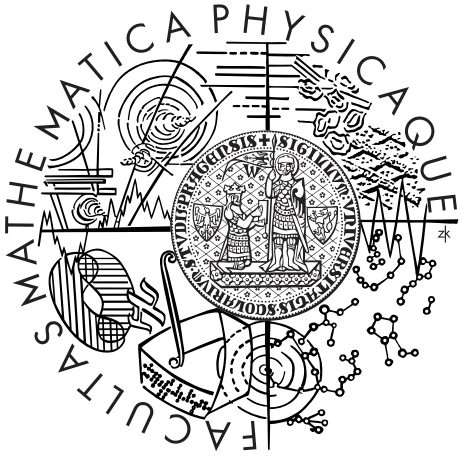

Michal Kloc

Kvantové kritické jevy v konečných systémech

Ústav částicové a jaderné fyziky

Vedoucí diplomové práce: prof. RNDr. Pavel Cejnar, Dr., DSc.
Studijní program: Fyzika
Studijní obor: Jaderná a subjaderná fyzika

Praha 2013

Charles University in Prague
Faculty of Mathematics and Physics

MASTER THESIS

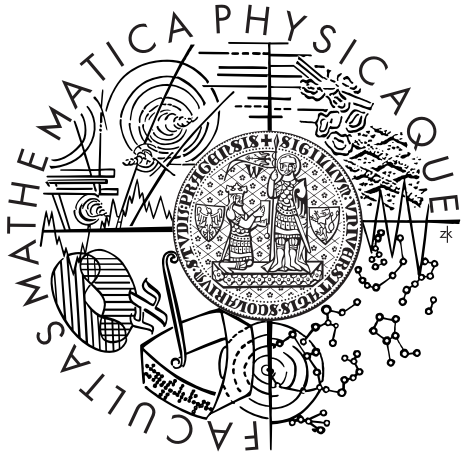

Michal Kloc

Quantum Critical Phenomena in Finite Systems

Institute of Particle and Nuclear Physics

Supervisor of the master thesis: prof. RNDr. Pavel Cejnar, Dr., DSc.
Study programme: Physics
Specialization: Nuclear and Subnuclear Physics

Prague 2013

Na tomto místě bych rád poděkoval vedoucímu své diplomové práce, prof. Pavlu Cejnarovi, za příkladné vedení, čas strávený diskuzemi nad fyzikální problematikou i čas věnovaný korekturám prvotních textů. Za další patří mé díky doc. Stanislavu Danišovi za pomoc s programem GNU Octave. V neposlední řadě si zaslouží obrovské poděkování má rodina a přátelé, bez jejichž podpory by tato práce jen těžko vznikla.

I declare that I carried out this master thesis independently, and only with the cited sources, literature and other professional sources.

I understand that my work relates to the rights and obligations under the Act No. 121/2000 Coll., the Copyright Act, as amended, in particular the fact that the Charles University in Prague has the right to conclude a license agreement on the use of this work as a school work pursuant to Section 60 paragraph 1 of the Copyright Act.

In Prague, April 12th, 2013 Michal Kloc

Název práce: Kvantové kritické jevy v konečných systémech

Autor: Michal Kloc

Katedra: Ústav částicové a jaderné fyziky

Vedoucí diplomové práce: prof. RNDr. Pavel Cejnar, Dr., DSc., Ústav částicové a jaderné fyziky

Abstrakt: Singularity v kvantových spektrech - kvantové fázové přechody základního či excitovaných stavů - jsou často spojeny se singularitami klasické limity systému a projevují se také na dalších charakteristikách, jako např. kvantové provázanosti. V první části práce studujeme kvantové fázové přechody v Lipkinově modelu, založeném na algebře $U(2)$. Je ukázán vztah mezi kvazistacionárními body klasického potenciálu a odpovídajícími singularitami v kvantových spektrech. V druhé části studujeme systém dvoustavových atomů interagujících s elektromagnetickým polem v optické dutině ve dvou zjednodušených modelech (neintegrabilním Dickeho modelu a jeho integrabilní verzi, známé jako Jaynesův-Cummingsův model). Je analyzováno chování kvantové provázanosti v těchto modelech se zřetelem na oblast v blízkosti fázových přechodů.

Klíčová slova: Kvantové fázové přechody, Kvantové fázové přechody excitovaných stavů, Kvantová provázanost

Title: Quantum Critical Phenomena in Finite Systems

Author: Michal Kloc

Department: Institute of Particle and Nuclear Physics

Supervisor: prof. RNDr. Pavel Cejnar, Dr., DSc., Institute of Particle and Nuclear Physics

Abstract: Singularities in quantum spectra - ground state and excited-state quantum phase transitions - are often connected with singularities in the classical limit of the system and have influence on other properties, such as quantum entanglement, as well. In the first part of the thesis we study quantum phase transitions within the $U(2)$-based Lipkin model. The relation between quasistationary points of the classical potential and the respective singularities in the spectrum is shown. In the second part, a system of two-level atoms interacting with electromagnetic field in an optical cavity is studied within two simplified models (non-integrable Dicke model and its integrable approximation known as Jaynes-Cummings model). The behaviour of quantum entanglement in these models is shown with a focus on the vicinity of the singular points.

Keywords: Quantum phase transitions, Excited-state quantum phase transitions, Quantum entanglement

Contents

Introduction

Quantum critical phenomena. Non-analytic properties of quantum spectra have been in the centre of interest in many fields of physics since 1970' when *quantum phase transitions* (QPTs) were introduced [1, 2]. QPTs can be recognized as singularities of the ground state for a certain critical value of a non-thermal control parameter λ_c when the size of the system is increased to infinity. Many systems that exhibit QPTs have been proposed and theoretically described as well as in numerous cases experimentally realized in various optical and solid-state models.

In recent years an analog of QPT for excited levels, so-called *excited-state quantum phase transition* (ESQPT), has been noted in certain many-body models [3, 4] which triggered a lot of new effort in this field. In particular, it turned out that the ESQPTs are related to some singularities in the classical phase space of the system, and that they may cause some thermodynamical anomalies.

Quantum entanglement. The non-separability of general quantum states describing composite quantum systems belongs to one of the most fascinating principles of the theory. Detailed knowledge of these purely quantum correlations is needed for understanding quantum technologies such as quantum computing. Anomalous behaviour of quantum entanglement has been recently associated with ground state QPTs [5]. However, there is a lack of knowledge about the behaviour of entanglement in excited states, especially in connection with ESQPTs. This is one of the main aims of this thesis.

The scheme of the thesis. In Chapter 1 we show some general properties of quantum spectra and introduce QPTs and ESQPTs. Then these phenomena are demonstrated in the Lipkin model. Chapter 2 is focused on the connection of quantum entanglement with QPTs and ESQPTs. Chapter 3 contains numerical study of selected optical models.

My own work was focused mostly on preparation, testing and subsequent use of computer codes which enable one to perform numerical calculations within several simple models that exhibit critical behaviour. The first part of these calculations is concentrated in Sec. 1.4. This section contains a pedagogical example of the Lipkin model. The second part comes in Sec. 2.3 and particularly in Chapter 3 where calculations within the Dicke and the Jaynes-Cummings models are performed. The calculations in the framework of the latter models are intended to be continued in a more systematic manner in our future work.

1. Non-analytic evolutions of quantum spectra

General form of the Hamiltonian. Throughout the thesis we consider Hamiltonians of a general form

$$\hat{H}(\lambda) = \hat{H}_0 + \lambda \hat{V}, \tag{1.1}$$

where $\hat{H}_0$ is the unperturbed part and $\hat{V}$ is the interaction. The real parameter $\lambda \in (-\infty, \infty)$ measures the strength of the interaction. Detailed description of various properties of such systems can be found in [6, 7, 8, 9], here we summarize the most significant ones.

The energy eigenproblem is given as $\hat{H}(\lambda)|n(\lambda)\rangle = E_n(\lambda)|n(\lambda)\rangle$. Naturally the relation of orthonormality for the eigenstates forming a basis of the relevant Hilbert space is given as

$$\langle m(\lambda)|n(\lambda)\rangle = \delta_{mn}. \tag{1.2}$$

We assume that $\hat{V}$ does not commute with $\hat{H}_0$

$$[\hat{H}_0, \hat{V}] \neq 0 \tag{1.3}$$

which is a reasonable assumption because otherwise the eigenstates of $\hat{H}$ and $\hat{H}_0$ would only differ in scaling. Any non-trivial evolution of eigenstates with a change of λ is given by the non-commutativity according to the equation (1.3). However this assumption is not necessary for the validity of the forthcoming formulas.

1.1 Level dynamics

Coulomb analogy. From the stationary perturbation theory one can derive information on the evolution of the energy levels with λ. Consider a perturbation $\hat{H}(\lambda + \delta\lambda) = \hat{H}(\lambda) + (\delta\lambda)\hat{V}$ where $\delta\lambda$ is sufficiently small. Then one can write the perturbative expansion

$$E_n(\lambda + \delta\lambda) = E_n(\lambda) + (\delta\lambda)V_{nn}(\lambda) + (\delta\lambda)^2 \sum_{m(\neg n)} \frac{|V_{mn}(\lambda)|^2}{E_n(\lambda) - E_m(\lambda)} \cdots \tag{1.4}$$

where we denoted $\langle m(\lambda)|\hat{V}|n(\lambda)\rangle \equiv V_{mn}(\lambda)$. Using Taylor expansion on the left hand side and comparing the terms with the same power of $(\delta\lambda)$ we obtain the following formulas

$$\frac{\mathrm{d}E_n(\lambda)}{\mathrm{d}\lambda} = V_{nn}(\lambda), \tag{1.5}$$

$$\frac{\mathrm{d}^2E_n(\lambda)}{\mathrm{d}\lambda^2} = 2\sum_{m(\neq n)} \frac{|V_{mn}(\lambda)|^2}{E_n(\lambda) - E_m(\lambda)}. \tag{1.6}$$

A similiar procedure where we use the perturbative expansion for eigenstates instead of energies

$$|n(\lambda + \delta\lambda)\rangle = |n(\lambda)\rangle + \sum_{m(\neq n)} \frac{V_{mn}(\lambda)}{E_n(\lambda) - E_m(\lambda)}|m(\lambda)\rangle \cdots \tag{1.7}$$

leads to the following:

$$\frac{\mathrm{d}V_{mn}(\lambda)}{\mathrm{d}\lambda} = \sum_{k(\neq m)} \frac{V_{mk}(\lambda)V_{kn}(\lambda)}{E_m(\lambda) - E_k(\lambda)} + \sum_{k(\neq n)} \frac{V_{mk}(\lambda)V_{kn}(\lambda)}{E_n(\lambda) - E_k(\lambda)}. \tag{1.8}$$

The common interpretation of the formulas (1.5), (1.6) and (1.8) is that individual levels behave as repelling charged particles with one degree of freedom [6, 7]. The energy of a particular level plays a role of a 'position' of a particle, $x_n \leftrightarrow E_n$, as well as diagonal terms of the disturbance, $V_{nn} \leftrightarrow p_n$, represent its 'momentum'. The 'product charges' of each pair of particles are propotional to the non-diagonal terms of the disturbance, $Q_{mn} \leftrightarrow V_{mn}$. This is also the weakest part of the interpretation because Q_{mn} cannot in general be factorized $Q_{mn} \neq Q_m Q_n$ and moreover depend nontrivially on λ (see (1.8)) which plays a role of 'time'.

Real and avoided crossings. The analogy with repelling charged particles gives a good intuitive picture of the behaviour of energy levels. Unless V_{nm} vanishes for some reasons, the closer the levels get, the stronger they repel. So the real crossing of levels is prohibited (except the cases to be discussed). This rule is known as *No-Crossing Theorem* (see Appendix A).

On the other hand for noninteracting levels, where $V_{nm} = 0$, real crossing is normal. If the condition is satisfied by each $m,\ n$, then the disturbance is of a diagonal form $\hat{V} = \mathrm{diag}\{p_1, p_2 \ldots, p_n\}$. However this is the case of $[\hat{H}_0, \hat{V}] = 0$ which we decided before not to take into account for its uninterestingness and unusualness. More generally we can consider a disturbance of a block diagonal form for all λ in a basis which diagonalizes $\hat{H}_0$. Then the corresponding Hilbert space splits into several subspaces on which the disturbance acts independently, so there is no interaction between these invariant subspaces. The crossings are possible for levels belonging to different subspaces.

Although the real crossings are rare, except the symmetry-dictated cases discussed above, quite often one can find places where levels get very close to each other. Such an event of sharp level collision is called *avoided crossing*.

It turns out to be useful to study the behaviour of eigenstates in the area of avoided crossing. Let's compute the probability of finding the eigenstate[1] $|n\rangle$ of the nth level of $\hat{H}(\lambda)$ in the eigenstate $|n'\rangle$ of the same Hamiltonian with a subtle change $\delta\lambda$, $\hat{H}(\lambda + \delta\lambda)$, of the same level.

$$\mathrm{Prob}(n'|n) = |\langle n'|n\rangle|^2 = \langle n'| \left(\mathbb{I} - \sum_{k(\neq n)} |k\rangle\langle k| \right) |n'\rangle = 1 - \sum_{k(\neq n)} |\langle n'|k\rangle|^2. \tag{1.9}$$

First order Taylor expansion gives $|n'\rangle \approx |n\rangle + \delta\lambda \frac{\partial}{\partial\lambda}|n\rangle$. From (1.7) along with the above mentioned Taylor expansion one can get the identity

$$\langle k| \left(\frac{\partial}{\partial\lambda}|n\rangle \right) = \frac{V_{kn}}{E_n - E_k} \quad \text{for } n \neq k. \tag{1.10}$$

When applied to (1.9) we obtain

[1] We do not write explicitly the λ dependence at this point.

$$\text{Prob}(n'|n) \approx 1 - (\delta\lambda)^2 \sum_{k\neq n} \frac{|V_{nk}|^2}{(E_n - E_k)^2}. \tag{1.11}$$

It is obvious that near the point of avoided crossing, where levels get very close to each other, even a small change of parameter λ results in a significant change of the wave function.

1.2 Quantum phase transitions

Ground-state phase transitions. The above described general rules play an important role in the formation of the spectrum. In this thesis we will deal with the systems which show a 'systematic' and (in some sense) 'coherent' occurence of avoided crossings. Moreover by increasing a parameter $\aleph$, quantifying the size of the system (see examples below), one can make these avoided crossings increasingly sharp, and in the limit $\aleph \to \infty$ non-analytic. We will call these phenomena *quantum phase transitions* (QPTs) [1, 2, 10, 11]. We will also show that QPTs can affect the ground state as well as excited states.

QPTs can be thought of as a generalization of classical thermodynamic phase transitions. However we consider interacting quantum objects at *zero temperature*, which undergo an abrupt change when the interaction parameter λ is varied. This implies that only properties of the ground state are taken into account. It is necessary to point out that the true QPTs occur only in the limit $\aleph \to \infty$. Within the system with finite $\aleph$ only some 'precursors' of QPTs can be observed. The value λ_c where such a transition occurs is called the critical point.

Ehrenfest classification. To classify QPTs one can employ the Ehrenfest's approach. The transitions of the *first kind* (discontinuous) are related to a discontinuity in the first derivative of energy with respect to the control parameter λ (also referred to as the first order QPTs). The phase transitions of the *second kind* (continuous) have the first derivative continuous whereas the non-analyticity (either a discontinuity or divergence) affects a higher-order derivative. For example the transition is of the kth Ehrenfest order, $k \geq 2$, if the kth derivative is discontinuous. In the case of a divergence in the kth derivative (instead of discontinuity) the transition has no Ehrenfest classification.

Excited-state quantum phase transitions. In generic situations the critical point is not separated and the QPT affects a certain region of the spectrum. These singularities in excited states are referred to as *excited-state quantum phase transitions* (ESQPTs) [1, 3, 4]. An ESQPT, in general, is a singularity in the scaled spectrum of the $\aleph \to \infty$ system along a certain critical borderline $E_c(\lambda)$ in the plane $\lambda \times E$, usually starting at the ground-state critical point. The type of the the singularity and the shape of $E_c(\lambda)$ depends on the specific system under study. Two manifestations of this phenomenon can be observed: First, singularities in level density $\rho(E)$ as a function of energy may appear accross the excited levels, second, the properties of the 'flow' of individual levels $E_i(\lambda)$ are affected when crossing the borderline (see Sec. 1.4).

1.3 Infinite vs. finite systems

Infinite systems. In a general many-body system the number of degrees of freedom is given by the number of constituents $\mathcal{N}$. So with the thermodynamic limit $\mathcal{N} \to \infty$ we are heading to the quantum-field description.

One can take a system of $\mathcal{N}$ $\frac{1}{2}$-spins as an example. The relevant Hilbert space $\mathcal{H} = \text{Span}\{|\updownarrow\rangle_1 |\updownarrow\rangle_2 \ldots |\updownarrow\rangle_{\mathcal{N}}\}$ naturally contains states with all possible total angular momenta

$$\mathcal{H} = C_{j_{min}}\mathcal{H}^{j_{min}}_{SU(2)} \oplus \ldots \oplus C_j\mathcal{H}^{j}_{SU(2)} \oplus \ldots \oplus C_{j=\frac{\mathcal{N}}{2}}\mathcal{H}^{j=\frac{\mathcal{N}}{2}}_{SU(2)} \tag{1.12}$$

where C_j stand for the numbers of possible coupling schemes of $\mathcal{N}$ spins into the total angular momentum j. The dynamical algebra of such a system, i. e. the algebra of all generators needed to build all relevant operators on $\mathcal{H}$, naturally consists of all the dynamical algebras of the individual spin subsystems $\oplus_{i=1}^{N} SU(2)_i \equiv \{\hat{j}_i^0, \hat{j}_i^{\pm}\}_{i=1}^{N}$, where $\hat{j}_i^{\bullet}$ stand for the Pauli matrices[2] at the ith spin site. Each spin unit adds two possibilities of the spin projection so in total one deals with $2^{\mathcal{N}}$ possible projections. Similarly, each spin unit adds one degree of freedom so for $\mathcal{N}$, naturally associated with $\aleph$, the number of degrees of freedom diverges in the limit $\mathcal{N} \to \infty$.

Finite systems. The framework in which this thesis is set is connected to the specific type of quantum systems that we will call *finite*[12]. The finiteness is related to a finite number of degrees of freedom which is independent on the size of the system which means that generally one describes some collective properties of the many-body system.

Again, we can use the spin system as an example but this time coupled to a maximal j, so the relevant Hilbert space[3] is

$$\mathcal{H} = \mathcal{H}^{j=\frac{\mathcal{N}}{2}}_{SU(2)} \text{ with dimension } d = 2j + 1 = \mathcal{N} + 1. \tag{1.13}$$

The related dynamical algebra is $SU(2) \equiv \{\hat{J}^0, \hat{J}^{\pm}\}$ where $\hat{J}^{\bullet} = \sum_{i=1}^{\mathcal{N}} \hat{j}_i^{\bullet}$. These 'collective' $SU(2)$ operators provide a non-local spin-spin interaction and so the global response of the system in the interaction with an outer system.

As another example, one may consider collective degrees of freedom of a nucleus. These are often described by models formulated in terms of a finite algebra of bosonic operators. The different types of bosons roughly corespond to different types of collective excitations, which define a certain finite number f of the degrees of freedom. This number remains constant irrespective of a possibly growing total number of bosons, $\mathcal{N}$, in the case of enlarging the valence nucleonic shell (the size of the nucleus).

To sum up [12], consider a finite dimensional dynamical algebra $\mathcal{G}$ of operators $\hat{G}_i,\ i = 1, 2 \ldots f$ where these operators serve as building elements of all relevant operators including the Hamiltonian $\hat{H} = \hat{H}(\hat{G}_i)$. The generators of $\mathcal{G}$ satisfy the closure relation $[\hat{G}_i, \hat{G}_j] = c_{ijk}\hat{G}_k$ where c_{ijk} are structure constants.

The difference of the finite systems from the ordinary many-body systems is the above noticed fact that the number of degrees of freedom does not grow with $\aleph$. This leads to the result that the infinite size limit is synonymous to classical limit. The

[2] Here we denote the z-Pauli matrix as $\hat{j}_i^0$.

[3] The coupling in this case is unique, so $C_{j=\frac{\mathcal{N}}{2}} = 1$.

latter conclusion can be justified [13] if one uses the scaled generators $\hat{g}_i = \hat{G}_i/\aleph^\kappa$ where $\kappa > 0$ is defined through consistent scaling $\hat{H}/\aleph = \hat{H}(\hat{G}_i/\aleph^\kappa)$ (for examples, see below). In the limit $\aleph \to \infty$ the commutators of the scaled generators vanish $[\hat{g}_i, \hat{g}_j] \to 0$ which justifies the term *classical limit*.

This implies that QPTs and ESQPTs in finite systems are always rooted in classical dynamics [3]. The first order QPTs are connected to the discontinuos development of the minimum of the potential in the configuration space with the control parameter λ. Similarly, the second order QPTs are connected to the development of the minimum whose trajectory (with varying λ) in the configuration space is continuous but non-analytic. For ESQPTs no classification has been established yet. However, their occurence in spectra is related to quasi-stationary points of the classical potential (local maxima or minima, inflection points, saddle points).

1.4 Example: Lipkin model

The Lipkin Hamiltonian. In this section we will demonstrate the phenomena related to QPTs and ESQPTs, respectively, on a simple $SU(2)$-based[4] Lipkin model [14]. We start with the Lipkin Hamiltonian in a so called Schwinger representation using two types of bosons *s* and *t*. For the respective annihilation and creation operators there are the commutation relations $[\hat{s}, \hat{s}^+] = [\hat{t}, \hat{t}^+] = 1$ while others are zero. To distinguish the two kinds of bosons we postulate the parity transformations $\hat{P}\hat{s}^+\hat{P}^{-1} = \hat{s}^+$ and $\hat{P}\hat{t}^+\hat{P}^{-1} = -\hat{t}^+$. We consider the Hamiltonian

$$\hat{H}^\chi_{\mathrm{L}}(\eta) = \eta\hat{n}_t - \frac{(1-\eta)}{N_{st}}\left(\hat{t}^+\hat{s} + \hat{s}^+\hat{t} + \chi\hat{t}^+\hat{t}\right)^2 \tag{1.14}$$

where $\eta \in [0,1]$ and $\chi \in (-\infty, \infty)$ are two free parameters[5]. The total number N_{st} of *s* and *t* is a conserved quantity. The presence of of N_{st} in the denominator of the interaction term follows from the requirement that the Hamiltonian 'behaves well' for $N_{st} \to \infty$ (see below). Without this scaling, the interaction term would completely dominate for very large N_{st}. The dimension of such a Hamiltonian is $d = N_{st} + 1$. We can rewrite (1.14) using the Schwinger mapping (see Appendix C)

$$\hat{J}_z = \frac{1}{2}\left(\hat{t}^+\hat{s} - \hat{s}^+\hat{t}\right), \quad \hat{J}_+ = \hat{t}^+\hat{s}, \quad \hat{J}_- = \hat{s}^+\hat{t}. \tag{1.15}$$

to the form

$$\hat{H}^\chi_{\mathrm{L}}(\eta) = \eta\left(\frac{N_{st}}{2} - \hat{J}_z\right) - \frac{(1-\eta)}{N_{st}}\left[\hat{J}_+ + \hat{J}_- + \chi\left(\frac{N_{st}}{2} - \hat{J}_z\right)\right]^2. \tag{1.16}$$

Obviously, this is an angular momentum form[6] of the Lipkin Hamiltonian with the dimension $d = 2j + 1$.

[4] A detailed discussion of general systems with $SU(2)$ dynamical algebra can be found in [15].

[5] Strictly speaking the presented Hamiltonian (1.14) is a generalized version to the parity conserving Lipkin model with defaultly $\chi = 0$.

[6] One can easily form $\hat{J}_x$ and $\hat{J}_y$ from the ladder operators according to the formulas $2\hat{J}_x = \hat{J}_+ + \hat{J}_-$ and $2i\hat{J}_y = \hat{J}_+ - \hat{J}_-$. Then it is straightforward to show that the $SU(2)$ commutation relation $[\hat{J}_i, \hat{J}_k] = i\varepsilon_{ijk}\hat{J}_k$ holds

Now, one can employ Holstein-Primakoff transformation [16] using only one type of bosons b

$$\hat{J}_z = \hat{b}^+\hat{b} - \frac{N_b^{\max}}{2}, \;\; \hat{J}_+ = \hat{b}^+\left(\sqrt{N_b^{\max} - \hat{b}^+\hat{b}}\right), \;\; \hat{J}_- = \left(\sqrt{N_b^{\max} - \hat{b}^+\hat{b}}\right)\hat{b} \quad (1.17)$$

where $N_b^{\max}$ is the maximal value of the *b*-bosons. So from (1.16) we arrive at the formula

$$\begin{aligned}\hat{H}_{\mathrm{L}}^{\chi}(\eta) &= \eta\left(\frac{N_{st} - N_b^{\max}}{2} + \hat{b}^+\hat{b}\right) - \frac{(1-\eta)}{N_{st}}\times \\ &\times\left[\hat{b}^+\left(\sqrt{N_b^{\max} - \hat{b}^+\hat{b}}\right) + \left(\sqrt{N_b^{\max} - \hat{b}^+\hat{b}}\right)\hat{b} + \chi\left(\frac{N_{st} - N_b^{\max}}{2} + \hat{b}^+\hat{b}\right)\right]\end{aligned} \quad (1.18)$$

Again, the dimension is $d = N_b^{\max}+1$, so we can conclude: $N_{st} = 2j = N_b^{\max} \equiv N$. Using this notation one can write

$$\begin{aligned}\hat{H}_{\mathrm{L}}^{\chi}(\eta) &= \eta\hat{b}^+\hat{b} - \frac{(1-\eta)}{N}\left[\hat{b}^+\left(\sqrt{N - \hat{b}^+\hat{b}}\right) + \left(\sqrt{N - \hat{b}^+\hat{b}}\right)\hat{b} + \chi\hat{b}^+\hat{b}\right]^2 \\ &= \eta\hat{b}^+\hat{b} - (1-\eta)\left[\hat{b}^+\left(\sqrt{1 - \frac{\hat{b}^+\hat{b}}{N}}\right) + \left(\sqrt{1 - \frac{\hat{b}^+\hat{b}}{N}}\right)\hat{b} + \chi\frac{\hat{b}^+\hat{b}}{\sqrt{N}}\right]^2\end{aligned} \quad (1.19)$$

At this point, we can use another transformation of the scaled operators $\hat{b}^+, \;\hat{b}$

$$\frac{\hat{b}^+}{\sqrt{N}} = \frac{\hat{x} - i\hat{p}}{\sqrt{2}}, \;\; \frac{\hat{b}}{\sqrt{N}} = \frac{\hat{x} + i\hat{p}}{\sqrt{2}}, \quad (1.20)$$

which leads to the commutation relation

$$[\hat{x}, \hat{p}] = i\frac{1}{N}. \quad (1.21)$$

Due to the boundedness of $\hat{b}^+\hat{b}$ in the interval $[0, N]$ we see that $\frac{x^2+p^2}{2}$ is bounded in $[0, 1]$.

Now we define scaled Hamiltonian[7] $\hat{\mathsf{h}} = \frac{\hat{H}}{N}$.

$$\begin{aligned}\hat{\mathsf{h}} &= \eta\frac{\hat{p}^2 + \hat{x}^2}{2} \\ &- (1-\eta)\left[\frac{\hat{x} - i\hat{p}}{\sqrt{2}}\sqrt{1 - \frac{\hat{p}^2 + \hat{x}^2}{2}} + \sqrt{1 - \frac{\hat{p}^2 + \hat{x}^2}{2}}\frac{\hat{x} + i\hat{p}}{\sqrt{2}} + \chi\frac{\hat{p}^2 + \hat{x}^2}{2}\right]^2\end{aligned} \quad (1.22)$$

The classical limit. By performing the limit $N \to \infty$ the commutation relation (1.21) vanishes ($\frac{1}{N}$ plays the role of Planck constant $\hbar$) and we obtain the classical limit $\hbar \to 0$

[7]Strictly speaking the new Hamiltonian represents a different system. However via an appropriate readjusting of the interaction strength one can restore the original Hamiltonian (1.19) for each value of N.

$$\begin{aligned}\mathsf{h}_{cl} = \eta\frac{p^2+x^2}{2} - 2\left(1-\eta\right)\left(1-\frac{p^2+x^2}{2}\right)x^2 \\ -\left(1-\eta\right)\left[2\chi\sqrt{2\left(1-\frac{p^2+x^2}{2}\right)}x\frac{p^2+x^2}{2} + \frac{\chi^2}{4}\left(p^2+x^2\right)^2\right].\end{aligned} \tag{1.23}$$

From the above explained restriction on x and p we see that the classical coordinates and momenta can be found only within the circle in the phase space of a radius $\sqrt{2}$. One may wish to find an appropriate canonical tranformation which 'stretches' $x \in [-\sqrt{2},\sqrt{2}]$ to $X \in [-\infty,\infty]$. A suitable transformation for x is [8]

$$X = \frac{x}{\sqrt{2-x^2}}. \tag{1.24}$$

The conjugate momentum P can be found using the condition that canonical transformation preserves Poisson brackets

$$\{X,P\} = \frac{\partial X}{\partial x}\frac{\partial P}{\partial p} - \frac{\partial P}{\partial x}\underbrace{\frac{\partial X}{\partial p}}_{=0} = 1. \tag{1.25}$$

So the solution for P is

$$P = \frac{\left(2-x^2\right)\sqrt{2-x^2}}{2+2x^2}p + C, \tag{1.26}$$

where C is a constant of integration which represents only a constant shift along the momentum-axis and can be set equal to zero.

Now we can use the inverse transformation $x = x(X),\ p = p(X,P)$ in (1.23) and express it via new variables. Our primary interest is the classical potential v_{cl} because its specific shape can be used to study QPTs so in the following we can omit the kinetic term (usualy very complicated) by setting $P = 0$.

$$\mathsf{v}_{cl} = \frac{\left(5\eta-4\right)X^2 - 4\left(1-\eta\right)\chi X^3 + \left[\eta-\left(1-\eta\right)\chi^2\right]X^4}{\left(1+X\right)^2}. \tag{1.27}$$

QPTs and ESQPTs. Here we present a numerical study of the spectra of the Lipkin Hamiltonian in four different setups. First we vary parameter η while χ being fixed, and then vice versa. In all the cases we work with $N = 50$.

Fig. 1.1 is a spectrum of the parity-conserving Lipkin Hamiltonian, i. e. $\chi = 0$. One can identify the QPT as the abrupt change of the ground state energy, marked 2), at $\eta = \frac{4}{5}$. One can also identify the ESQPT as a 'shockwave' in the excited states. Last but not least, we may notice that the 'nearly degenerate' states[8] at energies $E < 0$ become clearly distinguishable when crossing the critical borderline $E_c = 0$. The figure also contains the shapes of the classical potencial (1.27) corresponding to different values of η marked 1) to 4).

For $\eta = 1$, position 1), where the ground state consists of the s-boson condensate, the potential has a quadratic minimum. Then, when moving towards 2), the quartic

[8]For a degenerate double well potential (see 3) and 4) in Fig. 1.1) the levels lying deep in the wells are nearly degenerate, the tiny splitting being associated with quantum tunneling between the wells, which vanishes for $\hbar \to 0$.

term in the numerator begins to dominate and in the critical point 2), $\eta = \frac{4}{5}$, the minimum becomes purely quartic. The topology of the potentical changes dramatically at the point $X = 0$ and with a further change of η towards 3), a local maximum appears with two equally deep wells on both sides. Further development of η causes only deepening of both wells and does not change the shape of the potential qualitatively.

The structural change of the minimum of the potential is connected to the second order QPTs. When reaching the critical point, the ground state starts continuously propagating into the new minimum[9]. Similarly, when the higher-excitation levels reach the energy of the local maximum of v_{cl} (which can be associated with the borderline $E_c = 0$) the local level density suddenly grows (becoming singular in the thermodynamic limit).

As a second example of the level dynamics in the Lipkin model we present Fig. 1.2. Now, the parameter χ is varied, the value η being fixed as $\eta = 0.4$. So we proceed across the $\chi = 0$ line discussed in the previous example. Again, we present relevant shapes of v_{cl} for different values of the varied parameter. A remarkable difference from the previous case is that the potential does not change its structure qualitatively, only the mutual position and the relative depth of the minima is being changed. When crossing the critical point $\chi = 0$ the ground state undergoes the first order QPT as it jumps to the other well. In this case, three critical bordelines can be observed, forming a ∇-like shape in the spectrum. The upper line $E_c^{(1)} = 0$, which was present in the previous example too, is connected to the stationary point $X = 0$. The two lower borderlines $E_c^{(2)}(\chi)$ and $E_c^{(3)}(\chi)$ are connected with the respective secondary minimum of the potential. Together with $E_c^{(1)} = 0$ they separate the 'phase-coexistence region' in the energy interval defined by the vertical distance of both minima.

In the third setup (Fig. 1.3) we follow the development of the spectrum with η again, as in the first case, but this time for the parity-violating parameter $\chi = 0.5$. Obviously, the ground state goes through a phase transition with a similar manner as in Fig. 1.1 but the direct comparison would be misleading. One can show that for the parity-violating Lipkin Hamiltonian $\chi \neq 0$ the QPT is always of the first order [17]. Paradoxically, the behaviour of the ground state in the vicinity of the critical point is more similar to the situation in the second example. The position of the critical point η_c for general χ is [17]

$$\eta_c(\chi) = \frac{4 + \chi^2}{5 + \chi^2}. \tag{1.28}$$

In Fig. 1.4 we present the potential v_{cl} for $\eta_c(\chi = 0.5) \doteq 0.81$ with a zoom to the critical region. The two degenerate minina (although quite shallow) are present, the original one at $X = 0$ and the new one which grows deeper with further $\eta \to 0$.

Below $\eta = \frac{4}{5}$ the local minimum at $X = 0$ becomes a local maximum and a new secondary minimum appears at $X < 0$. Therefore, the potential is of a double-well kind again for $\eta \in [0, \frac{4}{5})$, but the separating barrier becomes much higher for decreasing η than in the case of Fig. 1.4. Due to the non-zero cubic term in (1.27) the two wells at $X < 0$ and $X > 0$ are not symmetric. As a consequence, two critical bordelines appear. The first one, $E_c^{(1)} = 0$, is the same as in the previous cases (again, associated with the local maximum of v_{cl}). The other one, $E_c^{(2)}(\lambda) = \mathsf{v}_{min}^{\mathrm{sec}}$, is associated with the secondary minimum of v_{cl}. The area between $E_c^{(1)}$ and $E_c^{(2)}(\eta)$ is a

[9] In the case when the wells are degenerate the ground state is a combination of states located in both wells.

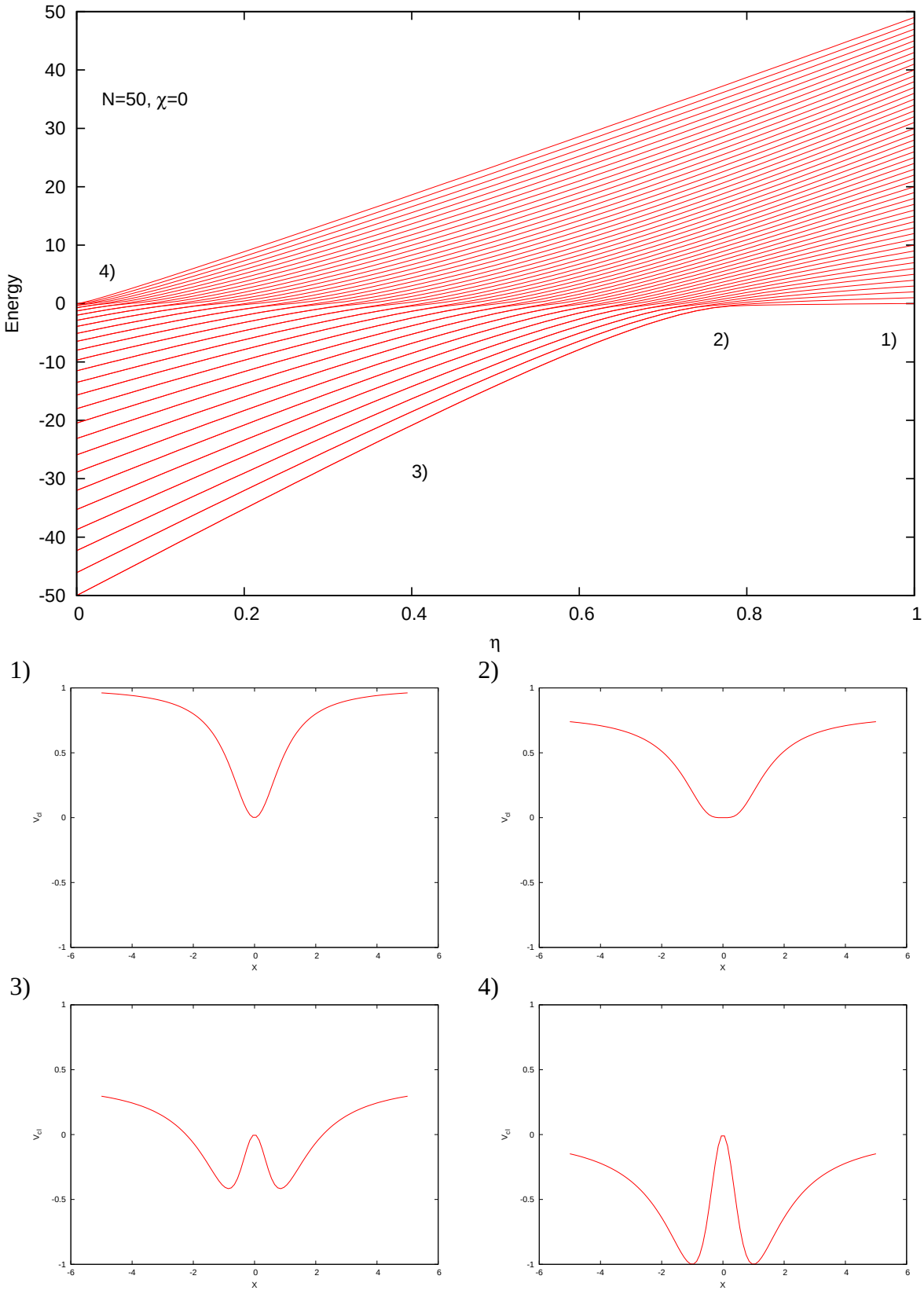

Figure 1.1: Energy spectrum of the Lipkin model in the first setup: $N = 50$, $\chi = 0$ and the shapes of the relevant classical potencial (1.27) for different values of η. Numbering is related to the position in the spectrum.

'mixed' phase consisting of avoided crossings of individual levels caused by tunneling between the two wells.

In the fourth setup the parameter $\eta = 0.9$ was fixed while χ being changed. This means that for $|\chi| < \sqrt{5}$ the global minimum of the potential is at $X = 0$. At $\chi = \pm\sqrt{5}$ a first order QPT appears, associated with the crossing of $X = 0$ and $X \neq 0$ minima. Accompanying ESQPTs are again present. A similar analysis as in the previous cases could be performed, however, here we present only the numerical results in Fig. 1.5. The interpretation in terms of the relevant shapes of v_{cl}, which are shown in Fig. 1.6, is left to the reader as an exercise.

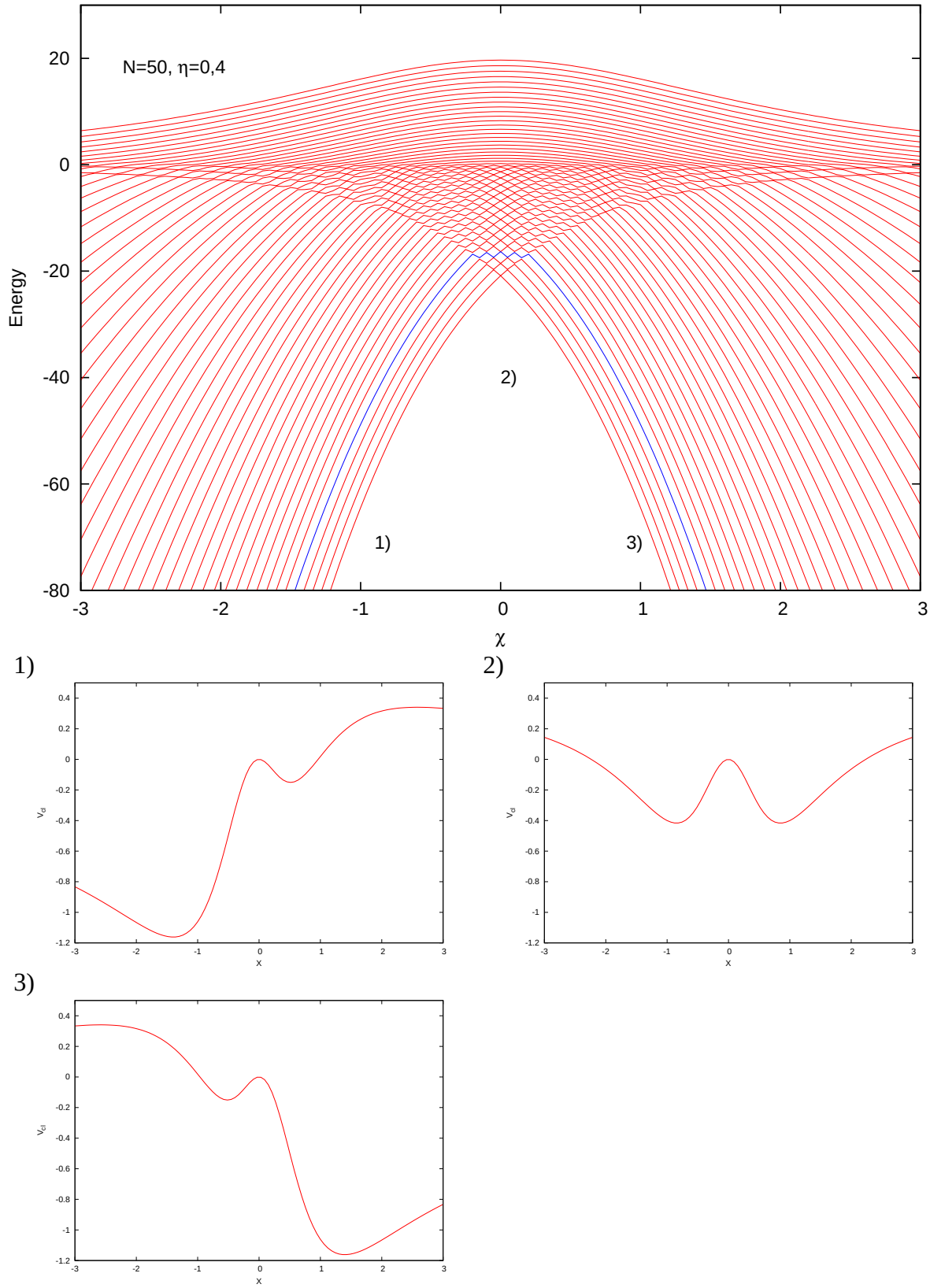

Figure 1.2: Energy spectrum of the Lipkin model in the third setup: $N = 50$, $\eta = 0.4$ and the shapes of the relevant classical potencial (1.27) for different values of χ. Numbering is related to the position in the spectrum. The blue colour of one of the levels highlights the avoided crossings in the spectrum.

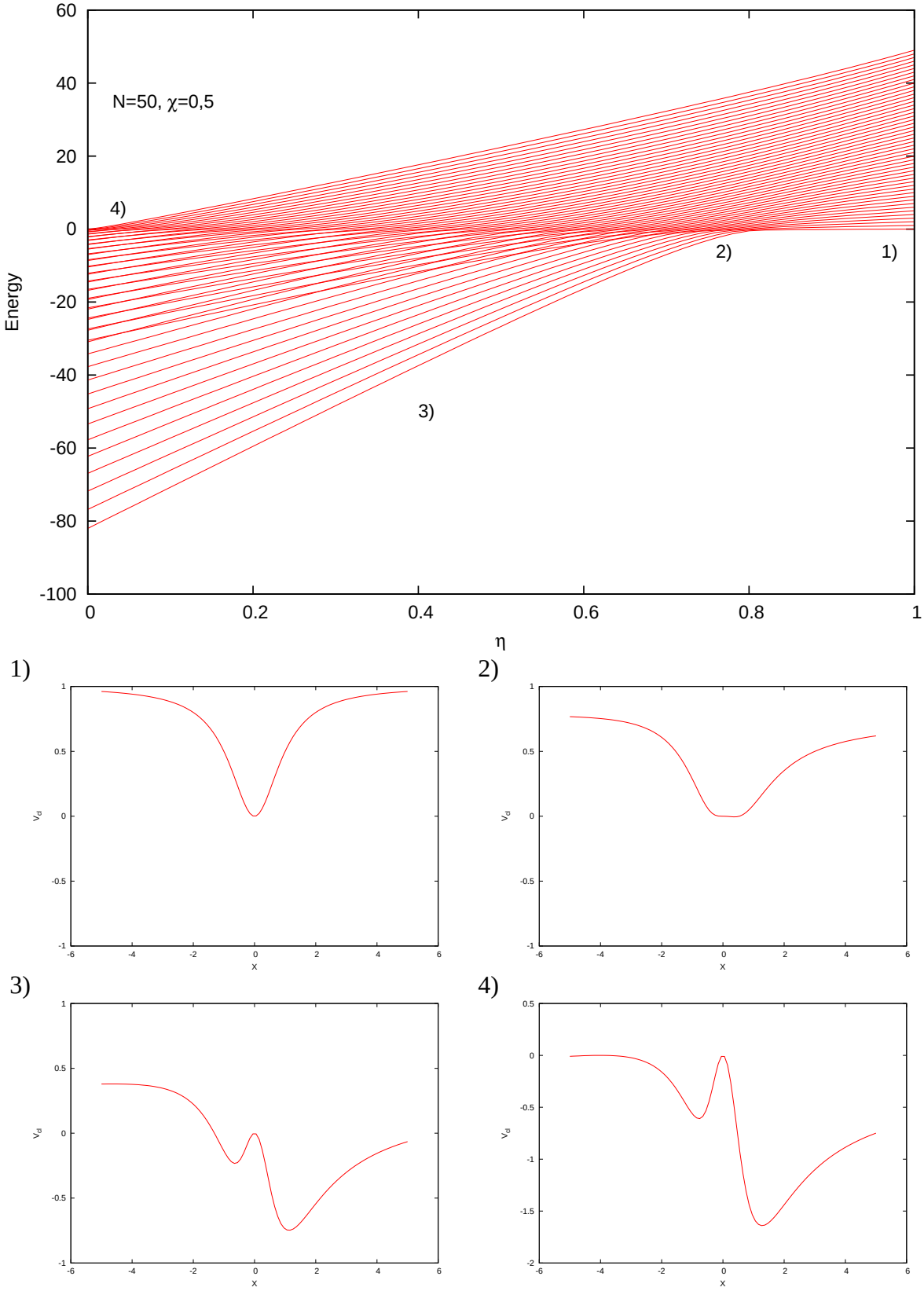

Figure 1.3: Energy spectrum of the Lipkin model in the second setup: $N = 50$, $\chi = 0.5$ and the shapes of the relevant classical potencial (1.27) for different values of η. Numbering is related to the position in the spectrum.

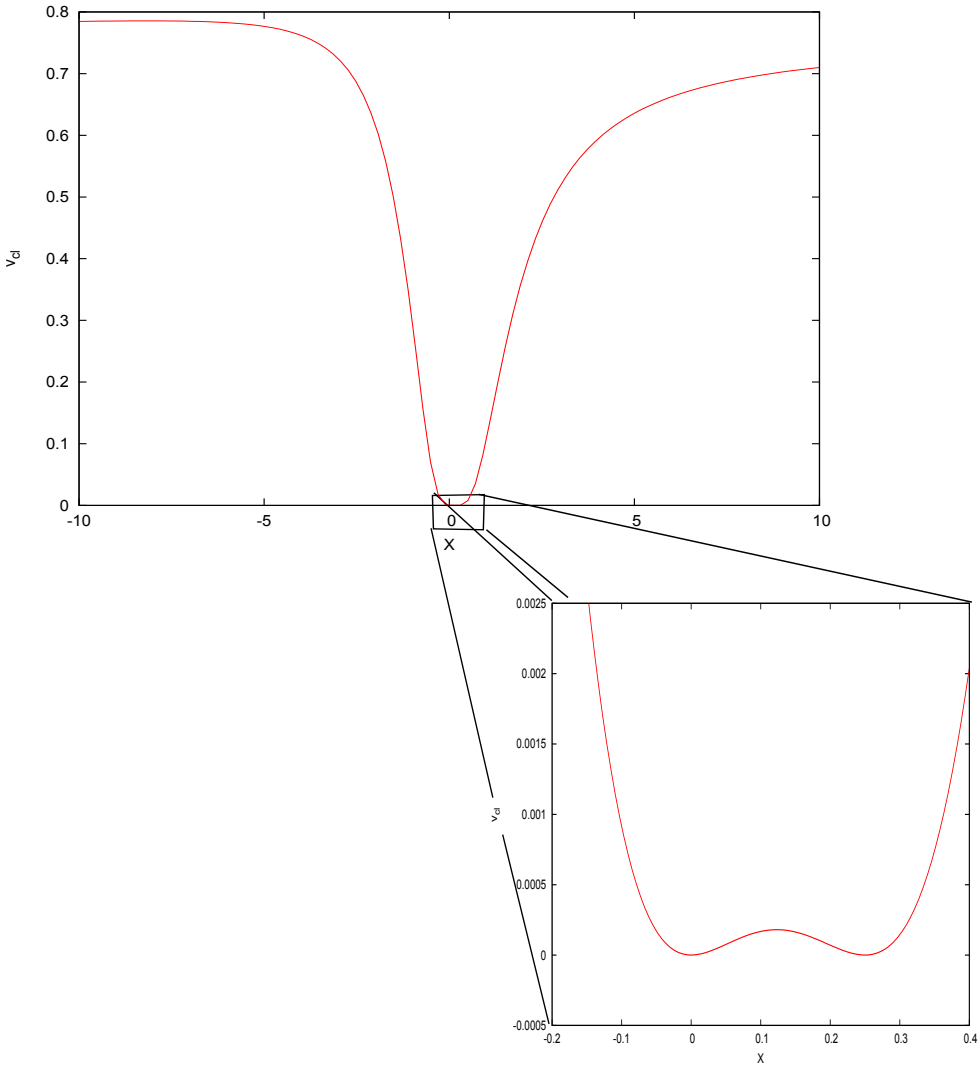

Figure 1.4: Classical potential (1.27) with a zoom in the critial point related to the spectrum in Fig. 1.3

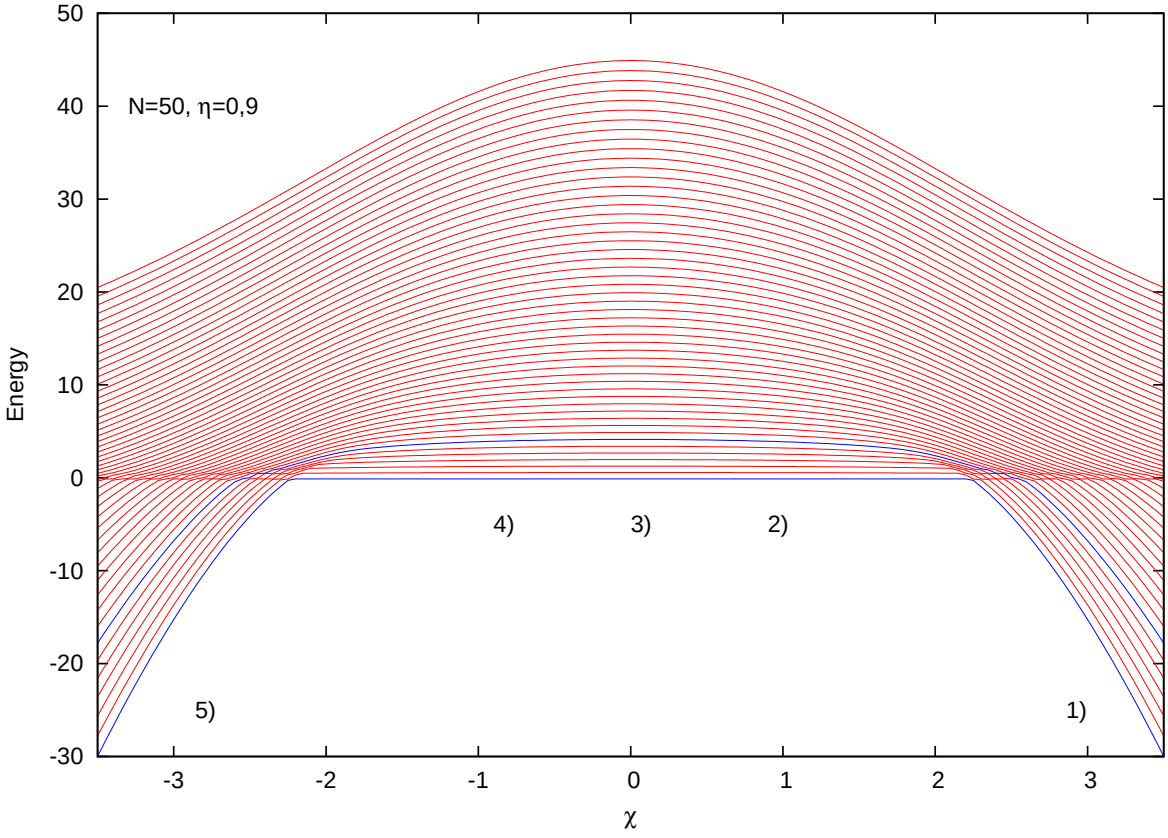

Figure 1.5: Energy spectrum of the Lipkin model in the fourth setup: $N = 50$, $\eta = 0.9$ and the shapes of the relevant classical potencial (1.27) for different values of χ. The blue colour of two of the levels serves as a guideline to highlight the development of individual levels in the spectrum.

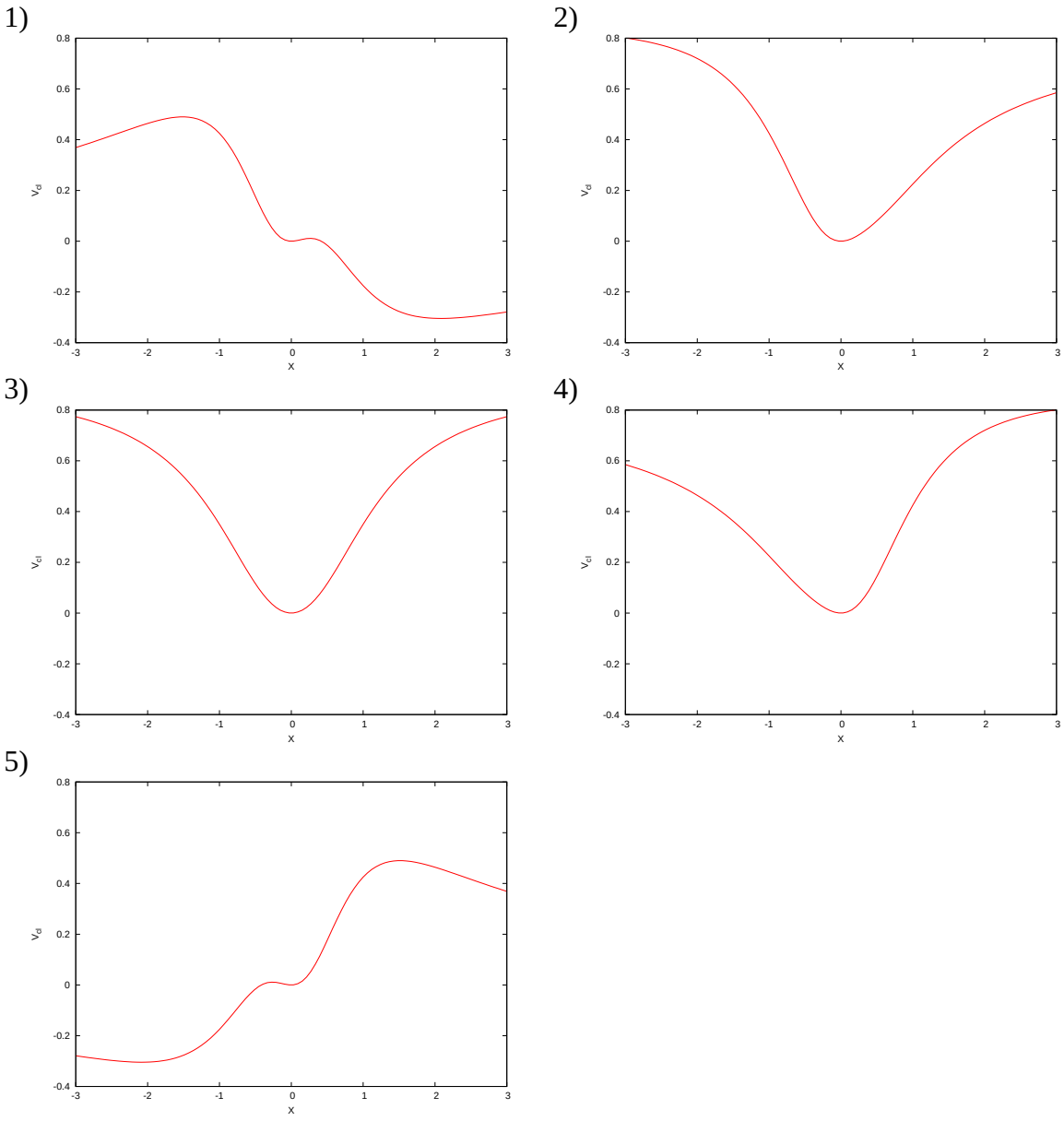

Figure 1.6: Potentials related to Fig. 1.5. Numbering is related to the position in the spectrum.

2. Quantum entanglement

Definition. Quantum entanglement and the non-locality of quantum mechanics as its direct consequence have been in the center of interest since the EPR-paradox was published [18]. This chapter is devoted to the description and the subsequent quantification of this quantum phenomenon. Its relevance for QPTs and ESQPTs will be discussed later.

Consider two Hilbert spaces $\mathcal{H}_{\mathrm{l}},\ \mathcal{H}_{\mathrm{r}}$ and the composite system given by the tensor product $\mathcal{H} = \mathcal{H}_{\mathrm{l}} \otimes \mathcal{H}_{\mathrm{r}}$. We denote orthonormal bases in $\mathcal{H}_{\mathrm{l}}$ and $\mathcal{H}_{\mathrm{r}}$ as $\{|\psi_{\mathrm{l}i}\rangle\}_{i=1}^{m}$ and $\{|\psi_{\mathrm{r}j}\rangle\}_{j=1}^{n}$ respectively, where $m = \dim\mathcal{H}_{\mathrm{l}}$ and $n = \dim\mathcal{H}_{\mathrm{r}}$. Obviously the dimension of the full Hilbert space $\mathcal{H}$ will be $\dim\mathcal{H} = m \cdot n$. Let $|\Psi\rangle$ be an arbitrary state in $\mathcal{H}$, one can expand it in terms of the natural basis $|\Phi_{ij}\rangle \equiv |\psi_{\mathrm{l}i}\rangle|\psi_{\mathrm{r}j}\rangle$

$$|\Psi\rangle = \sum_{i=1}^{m}\sum_{j=1}^{n}\gamma_{ij}|\Phi_{ij}\rangle \tag{2.1}$$

while the coefficients γ_{ij} generally cannot be simply factorized as $\gamma_{ij} = \alpha_i\beta_j$. Therefore one cannot write $|\Psi\rangle = |\psi_{\mathrm{l}}\rangle|\psi_{\mathrm{r}}\rangle$ where $|\psi_{\mathrm{l(r)}}\rangle \in \mathcal{H}_{\mathrm{l(r)}}$. This property of such systems is called *quantum entanglement*. It literally means that within a general state in $\mathcal{H}$ one cannot distinguish between 'the part from $\mathcal{H}_{\mathrm{l}}$' and 'the part from $\mathcal{H}_{\mathrm{r}}$' - together they form *the entangled state*.

2.1 Quantification

Description via density matrices. The full system can be equivalently treated using density matrix[1] $\hat{\rho} = |\Psi\rangle\langle\Psi|$. The way how to get information on the states of the individual subsystems is provided by partial trace technique

$$\begin{aligned}\hat{\rho}_{\mathrm{l}} = \mathrm{Tr}_{\mathrm{r}}\hat{\rho} = \sum_{k}\langle\psi_{\mathrm{r}k}|\Psi\rangle\langle\Psi|\psi_{\mathrm{r}k}\rangle = \sum_{ii'}\left(\sum_{j}\gamma_{ij}\gamma^{*}_{i'j}\right)|\psi_{\mathrm{l}i}\rangle\langle\psi_{\mathrm{l}i'}| = \\ = \sum_{ii'}\rho_{\mathrm{l}ii'}|\psi_{\mathrm{l}i}\rangle\langle\psi_{\mathrm{l}i'}|,\end{aligned} \tag{2.2}$$

$$\begin{aligned}\hat{\rho}_{\mathrm{r}} = \mathrm{Tr}_{\mathrm{l}}\hat{\rho} = \sum_{k}\langle\psi_{\mathrm{l}k}|\Psi\rangle\langle\Psi|\psi_{\mathrm{l}k}\rangle = \sum_{jj'}\left(\sum_{i}\gamma_{ij}\gamma^{*}_{ij'}\right)|\psi_{\mathrm{r}j}\rangle\langle\psi_{\mathrm{r}j'}| = \\ = \sum_{jj'}\rho_{\mathrm{r}jj'}|\psi_{\mathrm{r}j}\rangle\langle\psi_{\mathrm{r}j'}|,\end{aligned} \tag{2.3}$$

where we denoted $\rho_{\mathrm{l}ii'} = \left(\sum_j \gamma_{ij}\gamma^{*}_{i'j}\right)$ and $\rho_{\mathrm{r}jj'} = \left(\sum_i \gamma_{ij}\gamma^{*}_{ij'}\right)$. It can be shown that the operator $\hat{\rho}_{\mathrm{l}}$ on $\mathcal{H}_{\mathrm{l}}$ satisfies all the conditions imposed on density operator and so does $\hat{\rho}_{\mathrm{r}}$ on $\mathcal{H}_{\mathrm{r}}$ [19]. Obviously $\hat{\rho}_{\mathrm{l}}$ represents a pure state if and only if $|\Psi\rangle$ is of a special (separable) type $|\Psi\rangle = |\psi_{\mathrm{l}}\rangle|\psi_{\mathrm{r}}\rangle$.

[1] $|\Psi\rangle$ is a pure state on $\mathcal{H}$.

Entanglement entropy. There are several ways how to quantify entanglement of the system [20, 21]. One of them uses von Neumann's definition of entropy of the state described by the density matrix. Consider the density matrix $\hat{\rho} = \sum_i \rho_i |\phi_i\rangle\langle\phi_i|$ expressed via its eigenvalues ρ_i and orthonormal eigenvectors $|\phi_i\rangle$. Von Neumann entropy reads as

$$S(\rho) = -k_B \sum_i \rho_i \ln \rho_i = -\mathrm{Tr}\left[\hat{\rho} \ln \hat{\rho}\right]. \tag{2.4}$$

For pure states one gets $S = 0$ while for mixed states $S > 0$. The measure of entanglement in the state (2.1) can be naturally linked to the entropy $S(\rho_\mathrm{l})$ or $S(\rho_\mathrm{r})$ on the subsystems. This is often referred to as entanglement entropy $E(|\Psi\rangle)$. One can also show that the entanglement entropy is equal for the both subsystems $E(|\Psi\rangle) \equiv S(\rho_\mathrm{l}) = S(\rho_\mathrm{r})$. According to the Schmidt decomposition (see Appendix B) both $\hat{\rho}_\mathrm{l}$ and $\hat{\rho}_\mathrm{r}$ can be diagonalized with the same non-zero part of their eigenvalues. Therefore from (2.4) we obtain the same value of entropy for $\hat{\rho}_\mathrm{l}$ and $\hat{\rho}_\mathrm{r}$ as well.

However it should be remarked that such a simple link between the entropy of states on the subsystems with their entanglement fails if we consider a mixed state on $\mathcal{H}$[20]. The mixture is described by the density matrix

$$\hat{\rho} = \sum_i w_i |\Psi_i\rangle\langle\Psi_i| \tag{2.5}$$

where w_i are the probabilities of finding the system in the pure state $|\Psi_i\rangle$ (naturally adding up to one). It is necessary to keep in mind that decomposition (2.5) is *not* unique. Two different density matrices can describe the same system as well as we can perform the measurement in different bases[2]. The reduced density matrix $\hat{\rho}_\mathrm{l}$ can be computed as follows

$$\hat{\rho}_\mathrm{l} = \mathrm{Tr}_\mathrm{r}\hat{\rho} = \sum_{\xi=1}^{\dim\mathcal{H}} \sum_{i=1}^{\dim\mathcal{H}} w_i \sum_{\alpha\beta,\alpha'\beta'} \gamma^i_{\alpha\beta}\gamma^{*i}_{\alpha'\beta'} \underbrace{\langle\psi_{\mathrm{r}\xi}|\psi_{\mathrm{r}\beta}\rangle}_{\delta_{\xi\beta}} \underbrace{\langle\psi_{\mathrm{r}\beta'}|\psi_{\mathrm{r}\xi}\rangle}_{\delta_{\xi\beta'}} |\psi_{\mathrm{l}\alpha}\rangle\langle\psi_{\mathrm{l}\alpha'}| =$$

$$= \sum_{i=1}^{\dim\mathcal{H}} w_i \sum_{\alpha\beta,\alpha'} \gamma^i_{\alpha\beta}\gamma^{*i}_{\alpha'\beta} |\psi_{\mathrm{l}\alpha}\rangle\langle\psi_{\mathrm{l}\alpha'}| = \sum_{i=1}^{\dim\mathcal{H}} w_i \underbrace{\sum_{\alpha\alpha'} \left(\sum_\beta \gamma^i_{\alpha\beta}\gamma^{*i}_{\alpha'\beta} \right) |\psi_{\mathrm{l}\alpha}\rangle\langle\psi_{\mathrm{l}\alpha'}|}_{\equiv\hat{\rho}_{\mathrm{l}i}}$$

$$= \sum_{i=1}^{\dim\mathcal{H}} w_i \hat{\rho}_{\mathrm{l}i}.$$

So we obtain the density matrix $\hat{\rho}_\mathrm{l}$ in the form of linear combination of reduced density matrices related to the pure states $\{|\Psi_i\rangle\}$. Then the measure of entanglement is defined as the minimum over all decompositions of $\hat{\rho}$ [20, 21]

$$E(\hat{\rho}) = \min \sum_i w_i E(|\Psi_i\rangle). \tag{2.6}$$

Throughout the thesis we work only with pure states on $\mathcal{H}$ and so the above mentioned generalization does not have to be employed.

[2] One can choose different set of pure states $\{|\Psi'_i\rangle\}$. Generally we consider states such that $\langle\Psi_i|\Psi_i\rangle = 1$ but $\langle\Psi_i|\Psi_j\rangle \neq \delta_{ij}$

2.2 Hamiltonians producing entanglement

General interaction. One can consider Hamiltonian $\hat{H}$on $\mathcal{H} = \mathcal{H}_{\rm l} \otimes \mathcal{H}_{\rm r}$ of the form (1.1) which can be equally written as

$$\hat{H}(\lambda) = \hat{H}_{\rm l} \otimes \mathbb{I}_{\rm r} + \mathbb{I}_{\rm l} \otimes \hat{H}_{\rm r} + \lambda \sum_{i=1} \sum_{j=1} \Gamma_{ij} \hat{V}_{{\rm l}i} \otimes \hat{V}_{{\rm r}j} \tag{2.7}$$

where $\mathbb{I}$ is a symbol which stands for unit matrix. Operators $\hat{V}_{{\rm l}i}$ and $\hat{V}_{{\rm r}j}$ respectively, represent a set of independent Hermitian operators on $\mathcal{H}_{\rm l}$ and $\mathcal{H}_{\rm r}$ (e. g. the operators forming the respective spectrum generating algebra). So the most general interaction between the two subsystems, as used in (2.7), is a non-separable arbitrary combination of them with coefficients Γ_{ij}.

One can easily deduce that the entanglement of the state $|\Psi_n(\lambda)\rangle$, being an eigenstate of $\hat{H}(\lambda)$, can be computed according to the formula

$$E(|\Psi_n(\lambda)\rangle) = -{\rm Tr}\left[\hat{\rho}_{{\rm l}n}(\lambda) \ln \hat{\rho}_{{\rm l}n}(\lambda)\right] \tag{2.8}$$

where $\hat{\rho}_{{\rm l}n}$ is the reduced density matrix[3] related to $|\Psi_n(\lambda)\rangle$.

Now it can be easily shown that for the limit $\lambda \to 0$ the entanglement is zero. Let $|\xi_{\rm l}\rangle$ be an eigenstate of $\hat{H}_{\rm l}$ with eigenvalue ξ. Similarly, let $|\zeta_{\rm r}\rangle$ be an eigenstate of $\hat{H}_{\rm r}$ with eigenvalue ζ. In the limit $\lambda \to 0$, the eigenstates $|\Psi_n(0)\rangle$ are of the form of the simple tensor product $|\xi_{\rm l}\rangle|\zeta_{\rm r}\rangle$

$$\left(\hat{H}_{\rm l} \otimes \mathbb{I}_{\rm r} + \mathbb{I}_{\rm l} \otimes \hat{H}_{\rm r}\right) |\xi_{\rm l}\rangle|\zeta_{\rm r}\rangle = (\xi + \zeta)\, |\xi_{\rm l}\rangle|\zeta_{\rm r}\rangle. \tag{2.9}$$

Therefore for such separable states the entanglement entropy vanishes.

Separable interaction. Now, let us make a short note on the production of entanglement in this system with a *separable* interaction, in other words an interaction where $\Gamma_{ij} = \alpha_i \beta_j$

$$\sum_{i=1} \sum_{j=1} \Gamma_{ij} \hat{V}_{{\rm l}i} \otimes \hat{V}_{{\rm r}j} = \left(\sum_{i=1} \alpha_i \hat{V}_{{\rm l}i}\right) \otimes \left(\sum_{j=1} \beta_j \hat{V}_{{\rm r}j}\right) \equiv \hat{V}_{\rm l} \otimes \hat{V}_{\rm r}. \tag{2.10}$$

In this case, the eigenstates are generally entangled for finite λ but become separable for asymptotically growing $|\lambda|$. Apparently, the production of entanglement for finite values of λ is given by the non-commutativity of $\hat{H}_{\rm l}$ with $\hat{V}_{\rm l}$, and $\hat{H}_{\rm r}$ with $\hat{V}_{\rm r}$ respectively.

However, in the case $\lambda \to \infty$, the eigenstates of the Hamiltonian $\hat{H}(\lambda \to \infty)$ are constructed from the eigenstates of $\hat{V}_{\rm l}$ and $\hat{V}_{\rm r}$. We denote them $|v_{\rm l}\rangle$ and $|v_{\rm r}\rangle$ respectively. We also denote the respective eigenvalues as $v_{\rm l}$ and $v_{\rm r}$. So one can show easily

$$\hat{V}_{\rm l} \otimes \hat{V}_{\rm r}|v_{\rm l}\rangle|v_{\rm r}\rangle = v_{\rm l} v_{\rm r}|v_{\rm l}\rangle|v_{\rm r}\rangle. \tag{2.11}$$

So in the case of the separable interaction we arrive at the separable type of eigenstates of $\hat{H}(\lambda)$ in the limit $\lambda \to \infty$ with zero entanglement.

[3] Of course, one could use $\hat{\rho}_{{\rm r}n}$ as well.

2.3 Entanglement in QPTs

The anomalous bahaviour. The anomaly of entanglement in QPTs has been known since 2002 when A. Osterloh *et al* published the paper [5] . The idea was that the infinite correlation length, which occurs in the continuous theromodynamic phase transition, has a quantum counterpart in the description of QPT. A purely quantum correlation is represented by quantum entanglement.

Another paper by N. Lambert *et al* [22] followed up and showed that the entanglement grows extremely at the critical point for the ground state of the so called Dicke model (will be dicussed later in Chapter 3). In Fig. 2.1 we present our numerical results for the entropy of the ground state in the Dicke model which shows how the anomaly becomes sharper with the thermodynamic limit. This means that for the infinite size of the system (single mode radiation interacting with an ensamble of two-level atoms) the mutual entanglement of both subsystems (atoms vs. radiation) becomes singularly strong. The result is fully consistent with [22].

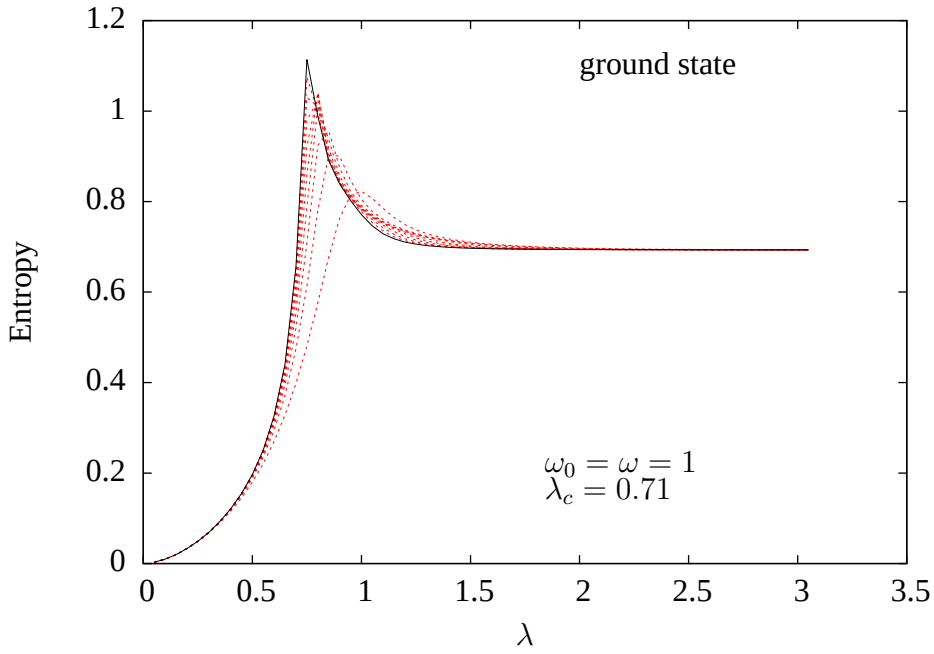

Figure 2.1: Entropy of the ground state of the Dicke model (see Sec. 3.1) for the different number of spin sites in the chain $N_{\text{spin}} = 5, 10, 15, 20, 25, 30, 40, 45, 50$.

Despite the number of papers on the anomal entanglement in QPTs none of them considers the behaviour of entanglement in ESQPTs. This is the crucial part of the forthcoming chapter.

3. Numerical study of entanglement

Optical models. In Chapter 1 we studied the Lipkin model in detail. However, in order to study the behaviour of entanglement in QPTs and ESQPTs, it is useful to consider systems with clearly defined subsystems which would eventually get entangled. For this reason we leave the Lipkin model and move towards some optical ones describing schematically the interaction of matter with electromagnetic field in a cavity. The matter is represented by an ensamble of two-level atoms whereas the radiation is approximated by one of its modes only. We will consider two versions of this setup, namely the Dicke and Jaynes-Cummings models.

3.1 Dicke model

The Dicke Hamiltonian. The Dicke model [23] describes the interaction of a chain of two-level atoms (or $\frac{1}{2}$-spin chain equivalently) with a quantized field of single-mode bosons (photons) in a optical cavity. The Dicke Hamiltonian is

$$\hat{H}_{\mathrm{D}} = \omega_0 \hat{J}_0 + \omega \hat{b}^+ \hat{b} + \frac{\lambda}{\sqrt{4j}} \left(\hat{b} + \hat{b}^+\right) \left(\hat{J}_- + \hat{J}_+\right), \tag{3.1}$$

where ω_0 and ω are single-particle energies[1], $\lambda \in [0, \infty)$ measures the interaction strength and $\hat{J}_0 \equiv \hat{J}_z$, $\hat{J}_\pm = \hat{J}_x \pm i\hat{J}_y$ satisfy the commutation relations of $SU(2)$ algebra

$$[\hat{J}_0, \hat{J}_\pm] = \pm \hat{J}_\pm, \quad [\hat{J}_+, \hat{J}_-] = 2\hat{J}_0. \tag{3.2}$$

For an array of $\frac{1}{2}$-spin sites the operators $\hat{J}_\bullet$ can be constructed as follows [13]:

$$\begin{aligned} \hat{J}_+ = \sum_{i=1}^{2j} \hat{a}^+_{\uparrow i} \hat{a}_{\downarrow i}, \quad \hat{J}_- = \sum_{i=1}^{2j} \hat{a}^+_{\downarrow i} \hat{a}_{\uparrow i}, \\ \hat{J}_0 = \frac{1}{2} \sum_{i=1}^{2j} \left(\hat{a}^+_{\uparrow i} \hat{a}_{\uparrow i} - \hat{a}^+_{\downarrow i} \hat{a}_{\downarrow i}\right), \end{aligned} \tag{3.3}$$

with $\hat{a}^+_{\uparrow i}$ or $\hat{a}_{\uparrow i}$ and $\hat{a}^+_{\downarrow i}$ or $\hat{a}_{\downarrow i}$ being creation or annihilation operators of spin-up and spin-down states of the fermion on site i (cf. the Lipkin model discussed in Sec. 1.4).

The single bosonic mode is given by the operators $\hat{b}^+$ and $\hat{b}$ often denoted as Heisenberg-Weyl algebra $HW(1)$ with a well-known commutation relation

$$[\hat{b}, \hat{b}^+] = 1. \tag{3.4}$$

The complete dynamical algebra[2] is then $SU(2) \otimes HW(1)$ so the Hilbert space consists of two clearly distinguishable subspaces of a spin chain and photons. The classical limit (including the potential) of the system can be constructed in a similar way as

[1] We set $\hbar \equiv 1$.

[2] Obviously, the system is one of those which we call finite because the dynamical algebra has a finite dimension.

described in Sec. 1.4 for the Lipkin model [13]. The system has two degrees of freedom, associated with both components of the dynamical algebra.

The scaling of the interaction term by $4j$, where $j = \frac{N_{\text{spin}}}{2}$ is the total angular momentum of the spin chain (naturally equal to the half of the number of spin sites), is necessary to keep the relative proportion of both terms when performing the thermodynamic limit here associated with $j \to \infty$.

QPTs and ESQPTs. The classical potential related to the Dicke model is two-dimensional. In general the system is *non-integrable*, i. e. unlike the Lipkin model with a certain conserved quantity removing one degree of freedom, there is no conservation-dictated constraint on the allowed combination of the basis vectors. For $\lambda = 0$ or for $\lambda > 0$ but sufficiently small, the ground state of the $j \to \infty$ system is associated with the boson vacuum combined with the lowest (for $\omega_0 > 0$) projection of the spin chain. When the interaction strength reaches the critical value $\lambda_c = \sqrt{\frac{\omega_0 \omega}{2}}$, the minimum of the potential becomes a saddle point [13]. At this point the superradiant phase is created which is characterized by a macroscopic excitation of both the bosonic field and the chain of spins. One can anticipate that such a structural transition results in a QPT of the second order in λ_c [24].

Because there are no finite dimensional irreducible representations which we could possibly work on (the spectrum has no upper bound), the truncation of the maximal number of photons must be performed in numerical diagonalization (see Appendix D). Note that the diagonalization is performed in $\lambda = 0$ eigenbasis which reads as $|n_b\rangle|m\rangle$, where n_b is the number of bosons (photons) and m is the projection of the spin chain (see Eq. 3.3).

In Fig. 3.1 we present Dicke spectra for two regimes: resonant and detuned, with N_{trunc} being a truncated number of photons in the system. In resonance $\omega_0 = \omega = 1$ the critical point is $\lambda_c = \frac{1}{\sqrt{2}}$, similarly for the detuned system $\omega_0 = 0.7$ and $\omega = 1.2$ the critical point is $\lambda_c \doteq 0.65$. One can clearly observe a QPT in λ_c in both cases. Despite the chaotic behaviour of the excited levels (which is a natural property of the non-integrable models), an ESQPT can be recognized as a non-analytic growth (with a diverging derivative) of level density developing with the saddle point of the two-dimensional potential for $\lambda > \lambda_c$ [22]. One can find some other structures in the excited level dynamics but their exact shape is slurred.

Entanglement. We used the entanglement entropy (2.4) to quantify the entanglement of the subsystems. The result for the ground state entropy development with λ was already shown in Fig. 2.1. The anomalous growth was obvious in a QPT, consistently with the earlier analysis [22].

The results for the excited-level dynamics (with entropy expressed via the colour scale) are in Fig. 3.2. Apparently, the behaviour of entanglement is complicated for excited states. Anyway, the Dicke interaction is of a separable type, as discussed in Sec. 2.2. So we can see that in both limits $\lambda \to 0$ and $\lambda \to \infty$ (see Fig. 3.3) the entanglement vanishes and so the both subsystems become decoupled. One can also estimate the area of the systematic entropy growth. The maximal entropy appears in a roughly triangular region located in between extrapolated lines corresponding to the ground state for $\lambda < \lambda_c$ and $\lambda > \lambda_c$. Note that one of these lines is the ESQPT critical borderline.

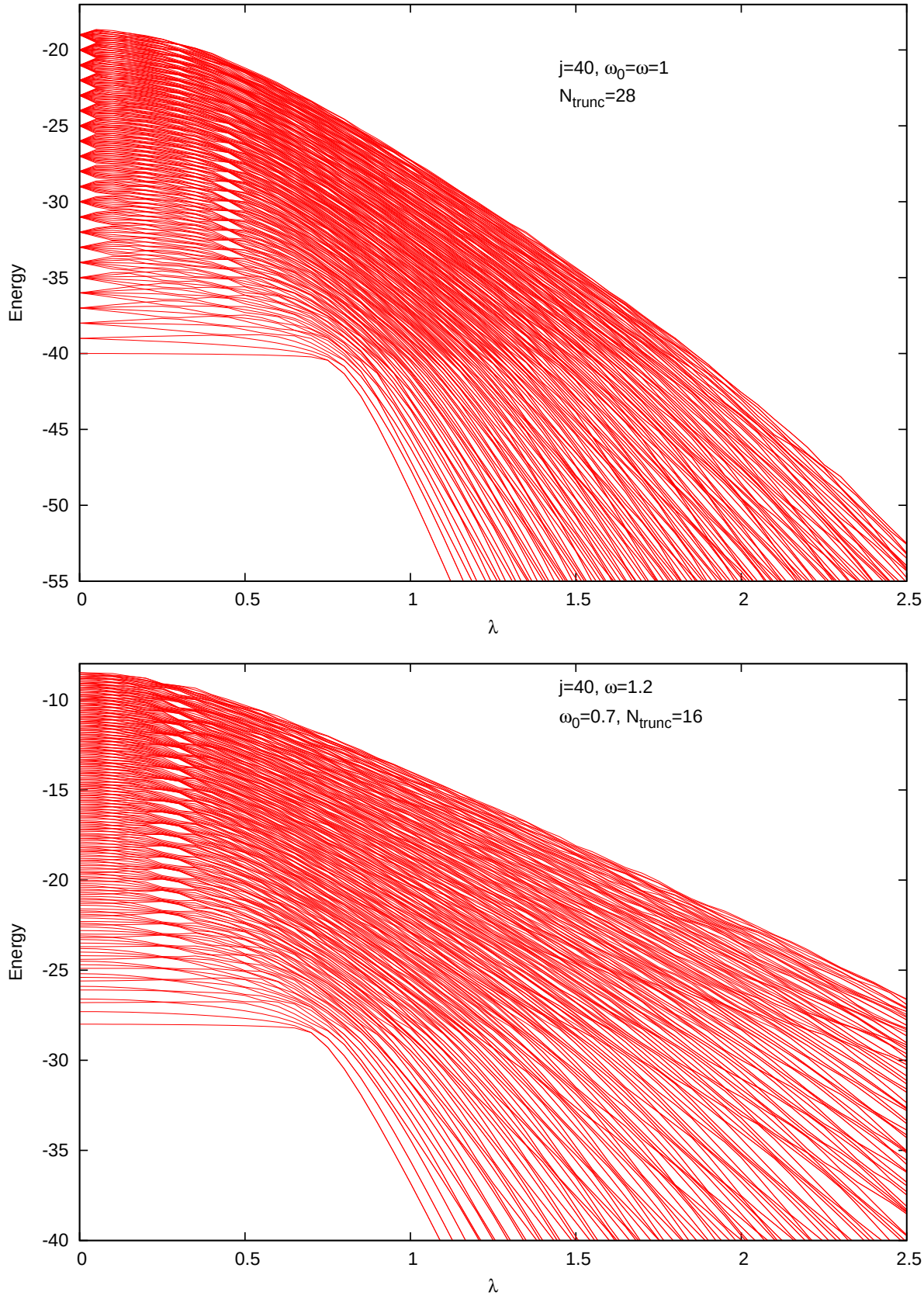

Figure 3.1: Energy levels of Dicke Hamiltonian with the length of the spin-chain $j = 40$ in resonance and detuned regime. Required number of relevant energy levels is 250.

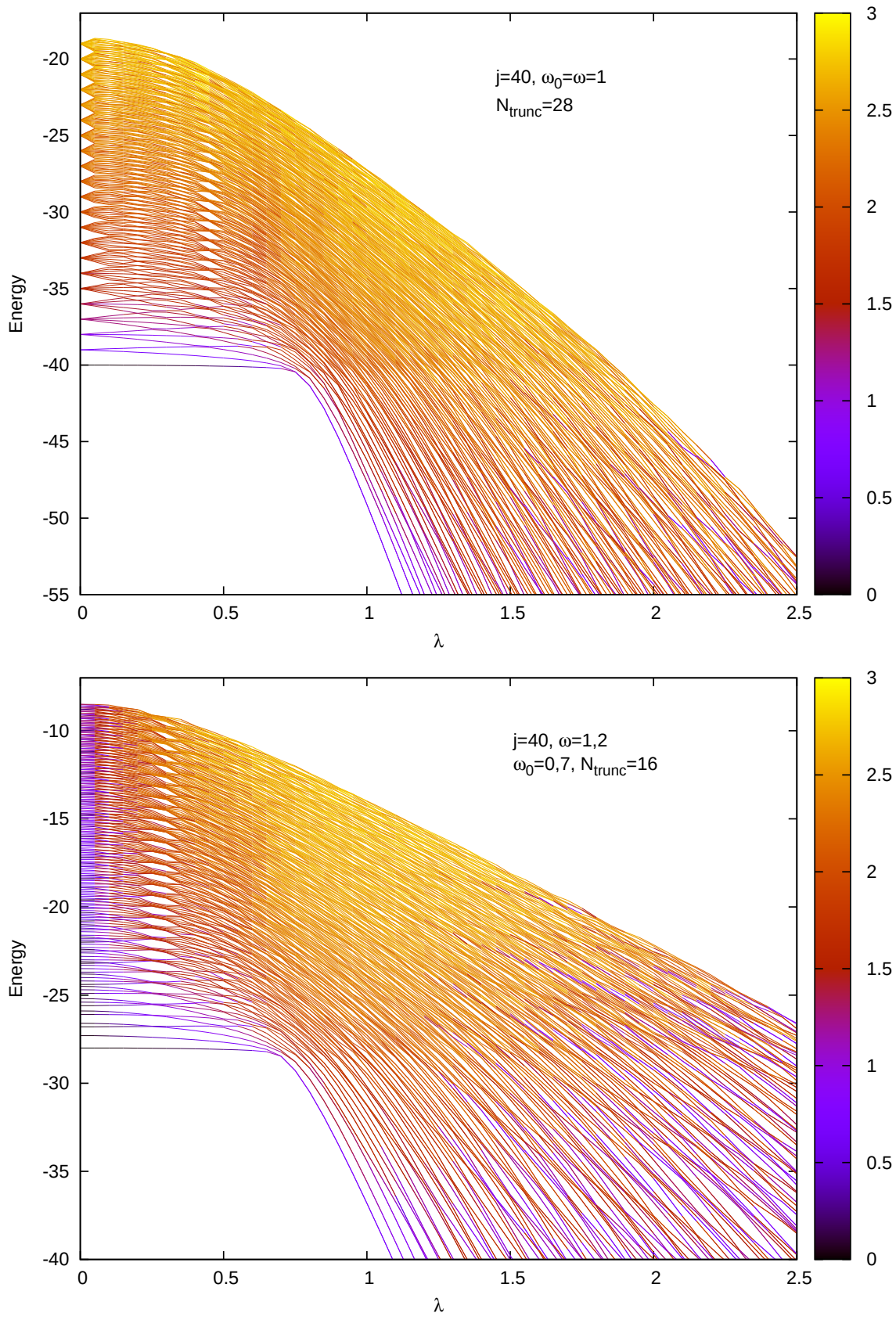

Figure 3.2: Energy levels with entropy (palette) of Dicke Hamiltonian in the same setup as in Fig. 3.1

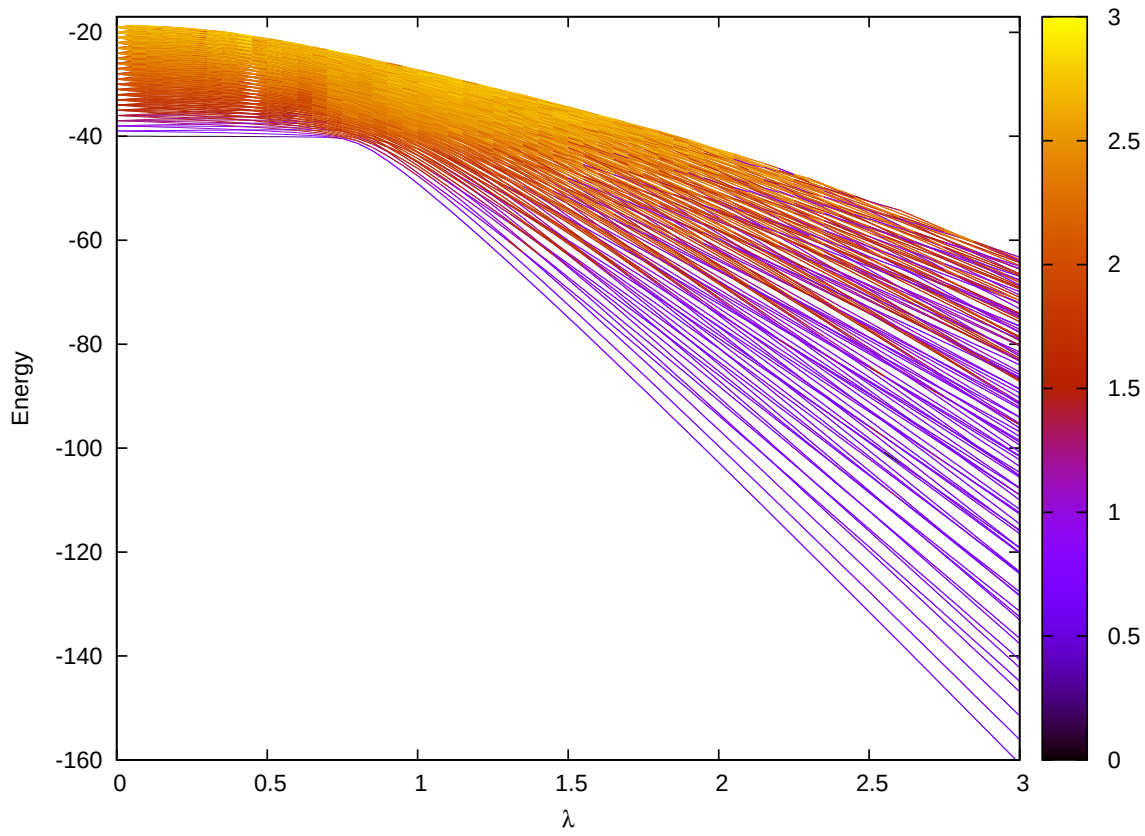

Figure 3.3: Energy levels with entropy (palette) of Dicke Hamiltonian in the resonance setup as in Fig. 3.1 with larger scale.

3.2 Jaynes-Cummings model

The Jaynes-Cummings Hamiltonian. This model is a frequently used *integrable* approximation of the Dicke model where $\hat{b}\hat{J}_-$ and $\hat{b}^+\hat{J}_+$ are omitted from the interaction term in (3.1) (see Appendix E for the so called *rotating wave approximation* - RWA). Then the Hamiltonian is

$$\hat{H}_{\text{JC}} = \omega_0\hat{J}_0 + \omega\hat{b}^+\hat{b} + \frac{\lambda}{\sqrt{M_{\text{JC}}}}\left(\hat{b}\hat{J}_+ + \hat{b}^+\hat{J}_-\right). \tag{3.5}$$

Note that we use a slightly different scalling of the interaction as used in [13]. The quantity M_{JC} is defined as $M_{\text{JC}} = 2\,(n_b + m + j)$. The integrability is conditioned by an existence of a conserved quantity removing one degree of freedom just like in the case of the Lipkin model. One can show that although the boson number n_b and the spin projection m are not conserved separately, their sum $n_b + m$ (hence also M_{JC}) is an integral of motion. So let us denote $\hat{N}_b \equiv \hat{b}^+\hat{b}$ counting the number of bosons. The sum $\hat{N}_b + \hat{J}_0$ commutes with Hamiltonian (3.5). Apparently, it commutes with the free part of the Hamiltonian (3.5) and it commutes with the interaction part as well, as can be shown explicitly

$$\hat{b}\hat{J}_+(\hat{N}_b + \hat{J}_0) = (\hat{N}_b + \hat{J}_0)\hat{b}\hat{J}_+ + \underbrace{[\hat{b}, \hat{N}_b]}_{\hat{b}}\hat{J}_+ + \hat{b}\underbrace{[\hat{J}_+, \hat{J}_0]}_{-\hat{J}_+} = (\hat{N}_b + \hat{J}_0)\hat{b}\hat{J}_+, \tag{3.6}$$

and similarly $\hat{b}^+\hat{J}_-(\hat{N}_b + \hat{J}_0) = (\hat{N}_b + \hat{J}_0)\hat{b}^+\hat{J}_-$.

The conservation of $\hat{N}_b + \hat{J}_0$ means that we always work within a finite subspace of boson states, therefore the overall number of states with given M_{JC} is also finite. The Hamiltonian eigenstates at $\lambda = 0$ are again of the form $|n_b\rangle|m\rangle$ as in the Dicke model, but only the allowed combinations with a fixed sum $n_b + m$ are possible, and in particular the ground state is not $|n_b = 0\rangle|m = -j\rangle$.

QPTs, ESQPTs and entanglement. In the forthcoming numerical solutions we consider a system with the number of spin sites equal to the maximal number of photons. In other words $M_{\text{JC}} = 4j$. We also asumme $\omega > \omega_0$ which means that we associate the $\lambda = 0$ ground state with the boson vacuum and fully excited spin chain $|n_b = 0\rangle|m = +j\rangle$. The classical analysis leads to a one-dimensional potential with a minimum that changes to a point of inflection in $\lambda_c = \frac{\Delta\omega}{\sqrt{2}}$ with $\Delta\omega = \omega - \omega_0$, where the ground state undegoes the second order QPT (see Fig. 3.4). The major part of the spectrum is 'laminar' but one can also observe a 'wave' of ESQPTs propagating from the critical point. In contrast to the analogous effect in the Lipkin model (Fig. 1.1), this 'coherent' growth of level density is connected with the development of the inflection point for $\lambda > \lambda_c$ [13]. We remind that at such a point, the level density has a singularity in the thermodynamic limit.

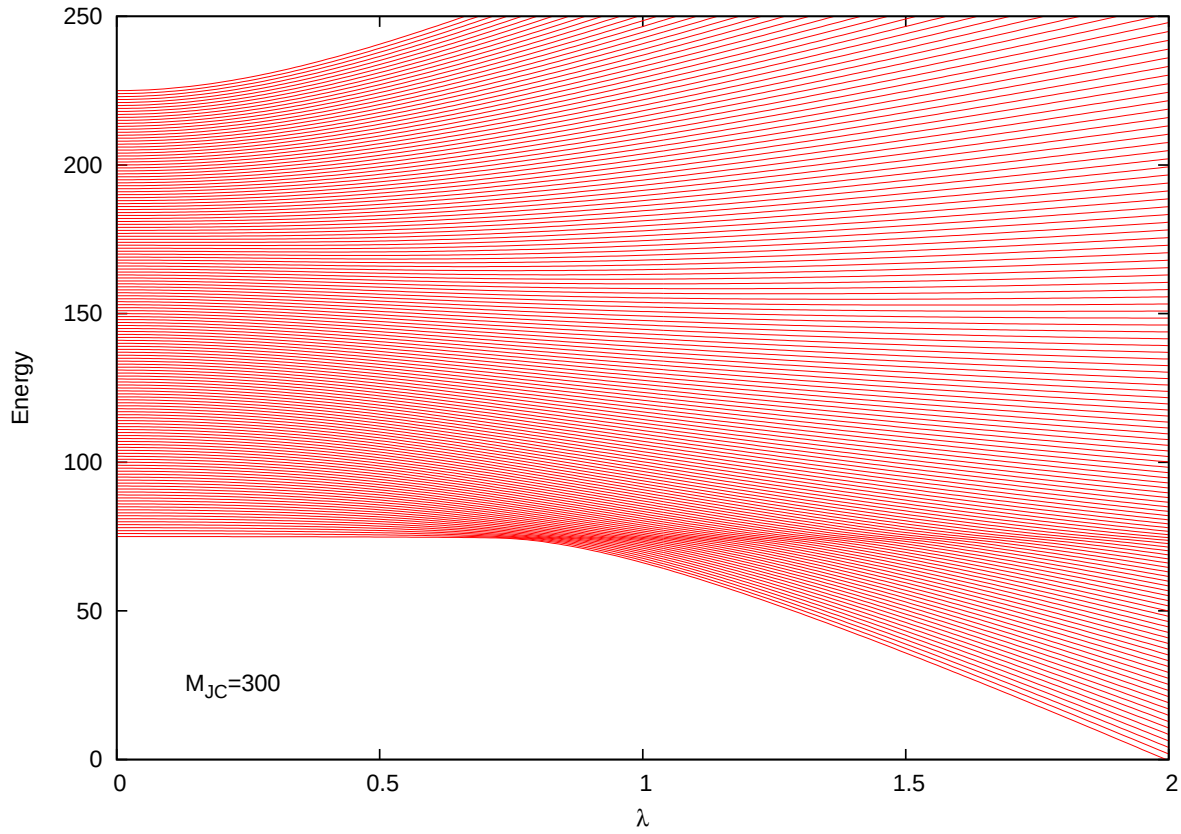

Figure 3.4: Energy levels of Jaynes-Cummings Hamiltonian with $M_{JC} = 300$, i. e. the number of spin sites is 150, $\Delta\omega = 1$, so the critical point for QPT is $\lambda_c = \frac{1}{\sqrt{2}}$.

The development of entanglement in the spectrum is in Fig. 3.5. One can clearly identify the area of systematically decreased entanglement close to the ESQPTs. The

behaviour of entropy of selected individual levels is in Fig. 3.6. The ground state entropy grows suddenly at critical λ_c. The similar growth can be noticed for excited states as well, however, the local minimum in entanglement starts progressing. This can be also noticed from Fig. 3.7.

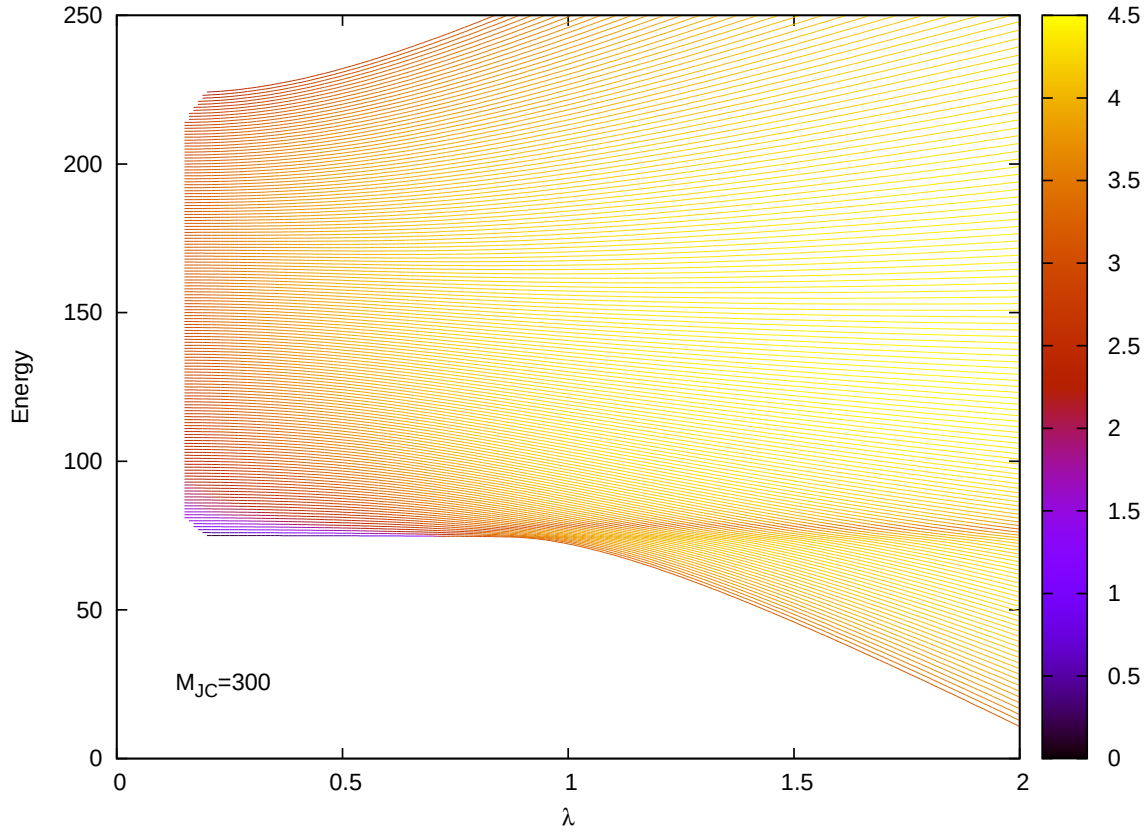

Figure 3.5: Energy levels and entropy (palette) for Jaynes-Cummings Hamiltonian in the same setup as Fig. 3.4

In Fig. 3.8 we show how individual-level entropy adds up to form some kind of 'collective' enveloping growth of entanglement. A few selected levels are put in green to highlight the individual shape and the way how they contribute to the collective envelope.

A more detailed explanation of the systematic evolution of entanglement will be a subject of the further study.

Comparison with the Dicke model. One may naturally wish to see the comparison of both used optical models as one is supposed to be an approximation of the other. In Fig. 3.9 we present our numerical results for energy levels. A similar picture can be found in [24]. The figure is a synthetis of several spectra of the Jaynes-Cummings Hamiltonian with a fixed length of the spin-chain j but for different $n_b^{\max}$ being the maximal number of photons in the system. One can notice that different values of $n_b^{\max}$ result in different values of M_{JC} (see Table 3.1). So changing $n_b^{\max}$ in the scale $n_b^{\max} = 0, 1, 2 \ldots$ leads to moving from one symmetry subspace to another in each step.

The straight horizontal line at energy -3.5 represents the trivial system with $M_{\text{JC}} = 0$. It consist of the spin chain with the projection $J_0 = -j$. So as there are no photons

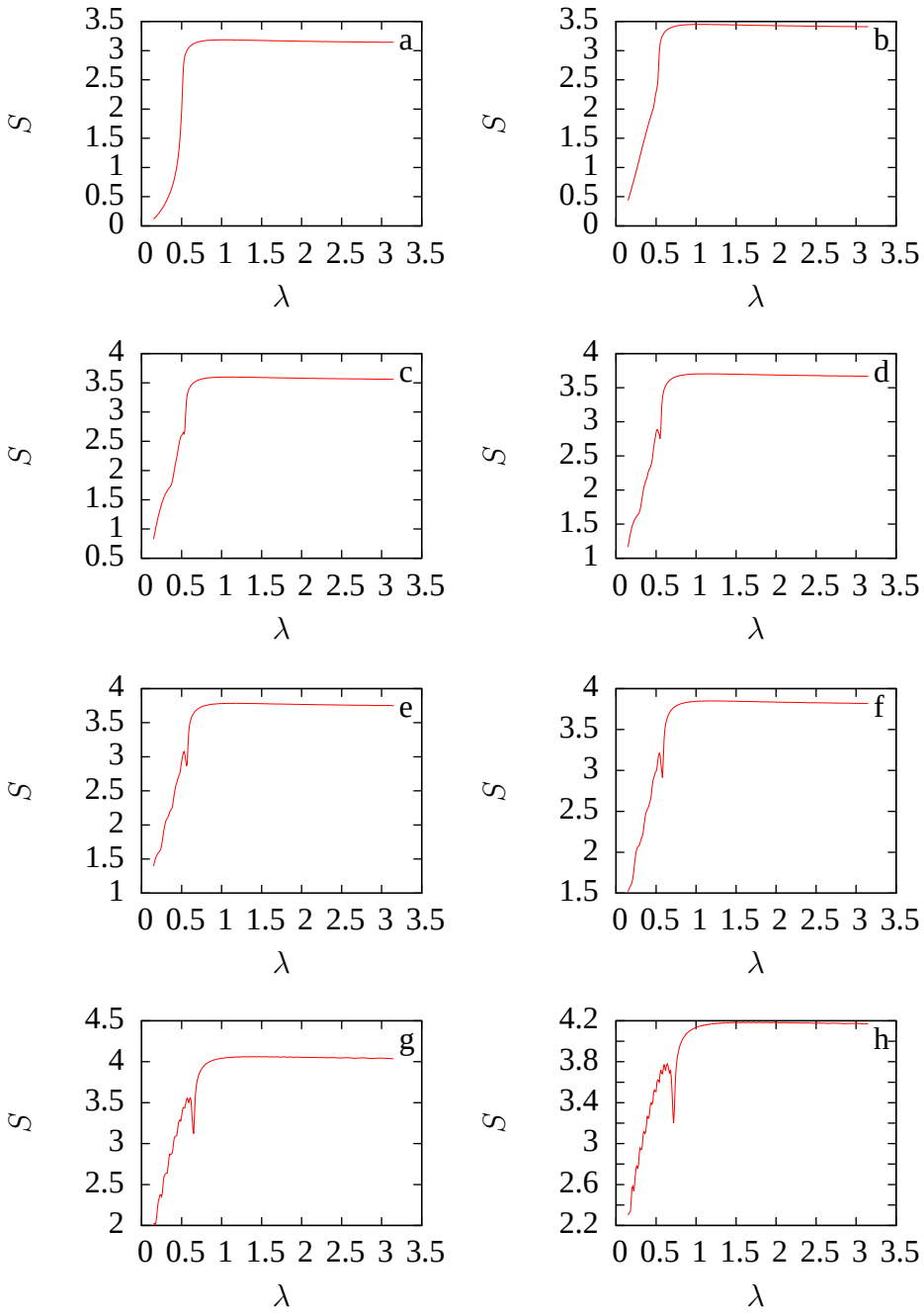

Figure 3.6: Entropy S of the Jaynes-Cummings model, *a*) Ground state, *b*) 1st excited, *c*) 2nd excited, *d*) 3rd excited, *e*) 4th excited, *f*) 5th excited, *g*) 10th excited, *h*) 15th excited. In this case $M_{JC} = 300$, i. e. the number of spin sites is 150, $\Delta\omega = 0,7$, which implies $\lambda_c = 0,5$.

to interact with, the state remains unchanged along the variation of λ. In the next step we take $M_{\mathrm{JC}} = 2$. Now, there are two possible states of such a system developing with λ. And so we can continue.

The individual lines form some visible structure where (at least) the one forming the lower bound can be associated with the ground state of the relevant Dicke model with a proper position of the critical point.

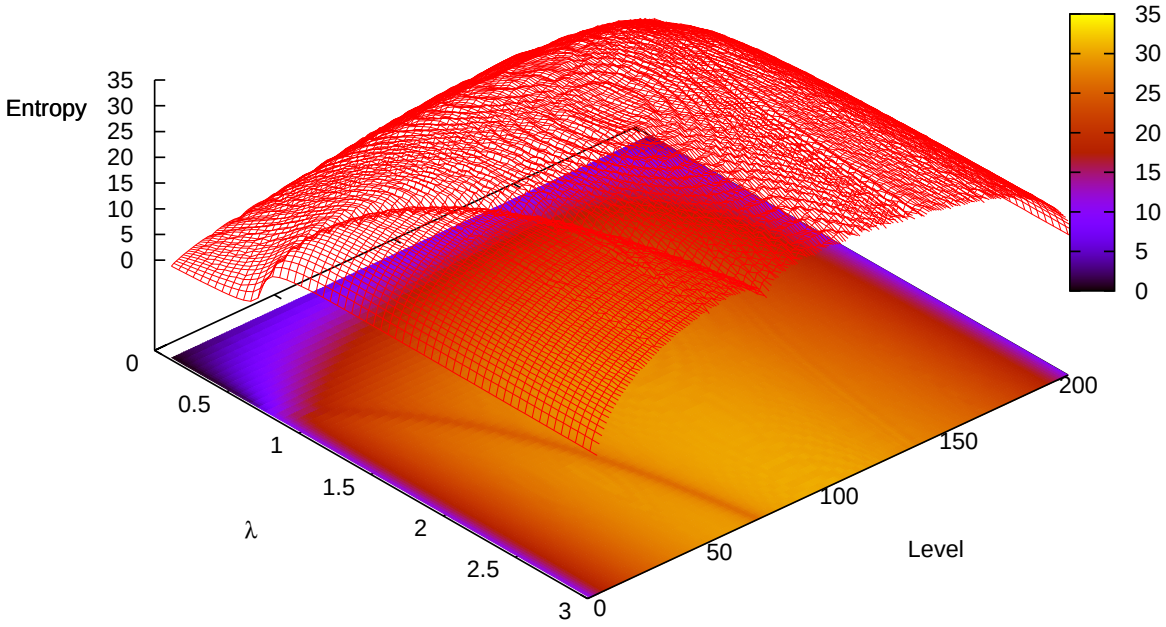

Figure 3.7: Entanglement entropy of the Jaynes-Cummings model as a function of λ and the ordinal number of the level, $M_{\mathrm{JC}} = 400$, i. e. the number of spin sites is 200, $\Delta\omega = 1$.

In Fig. 3.10 we present the direct comparison of the entanglement entropy in the Dicke spectrum with the equivalent RWA spectrum. The RWA spectrum is obviously not complete because in numerical computation we had to use only a bounded set of M_{JC} values. Anyway, our results still support the general idea that RWA is a relevant approximation for a rather small interaction strength [25] however for large λ the approximation fails. This can be seen for example from the fact that the Dicke interaction term is separable where (as discussed in Sec. 2.2) the both subsystems become decoupled in $\lambda \to \infty$ whereas in the case of non-separable interaction of the Jaynes-Cummings type, such a decoupling does not occur.

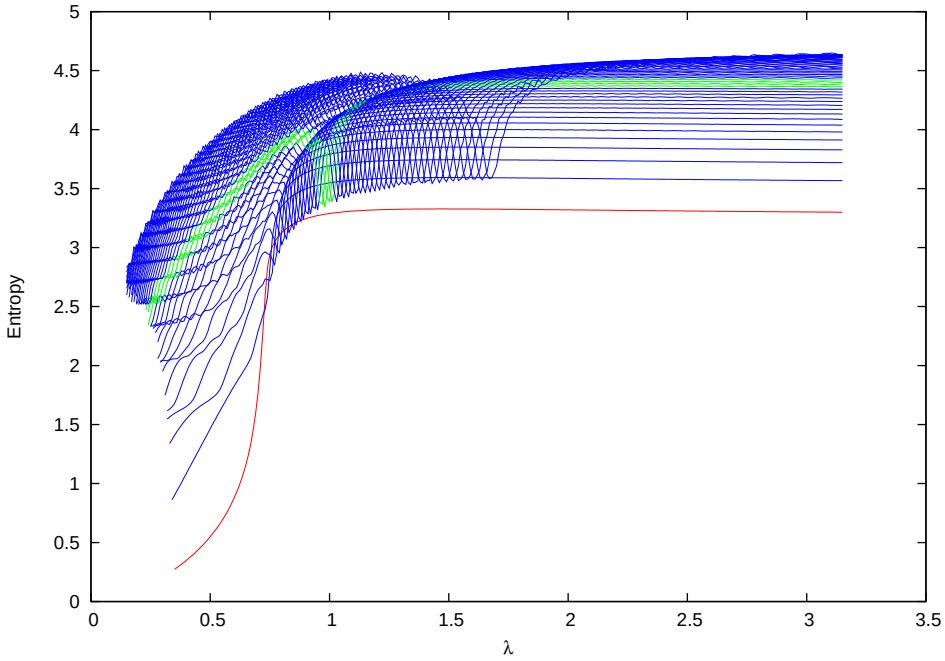

Figure 3.8: Development of the the entropy for individual levels, $M_{\text{JC}} = 400$, i. e. the number of spin sites is 200, $\Delta\omega = 1$. Ground state is put in red colour.

M_{JC}	n_b	m	dimension
0	0	$-j$	1
2	0	$-j+1$	2
	1	$-j$	
4	0	$-j+2$	3
	1	$-j+1$	
	3	$-j$	
$\vdots$			$\vdots$
$4j$	0	j	$2j+1$
	1	$j-1$	
	$\vdots$	$\vdots$	
	$j-1$	1	
	j	0	
$4j+2$	1	j	$2j+1$
	2	$j-1$	
	$\vdots$	$\vdots$	
	$j-1$	1	
	j	0	
$\vdots$			$\vdots$

Table 3.1: Possible combinations of n_b and m related to the same symmetry subspace M_{JC}. Note that M_{JC} is by definition even.

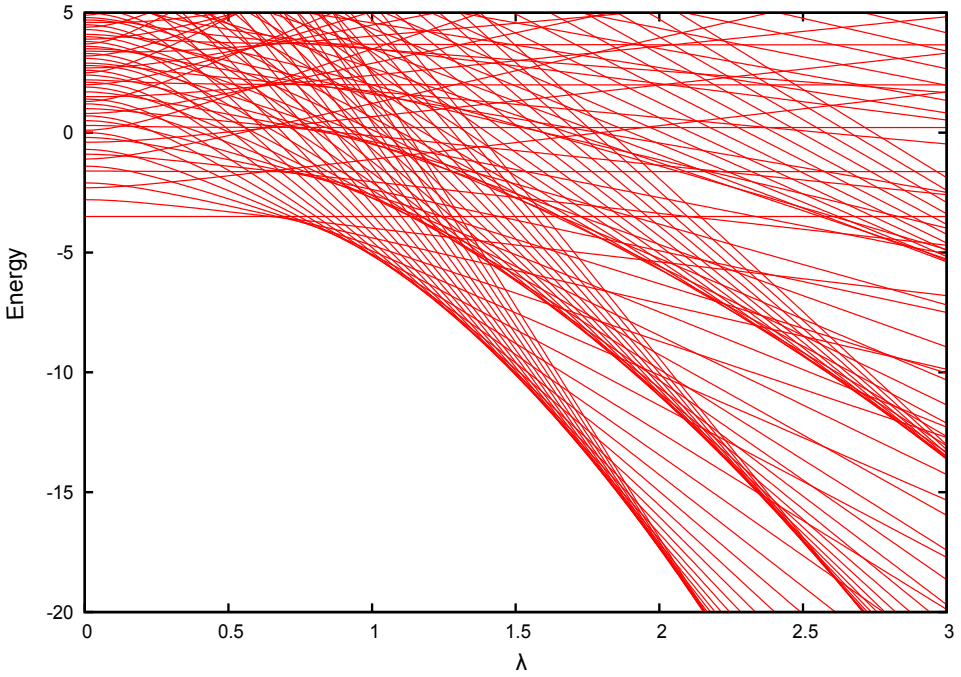

Figure 3.9: Energy spectra of the Jaynes-Cummings model ($\omega_0 = 0.7$, $\omega = 1.2$) for different M_{JC} with a fixed $j = 5$ forming an equivalent of a ground state QPT as in the Dicke model with the same j and the same single-particle energies as well. Note that levels belonging to different M_{JC} do cross as a consequence of symmetry.

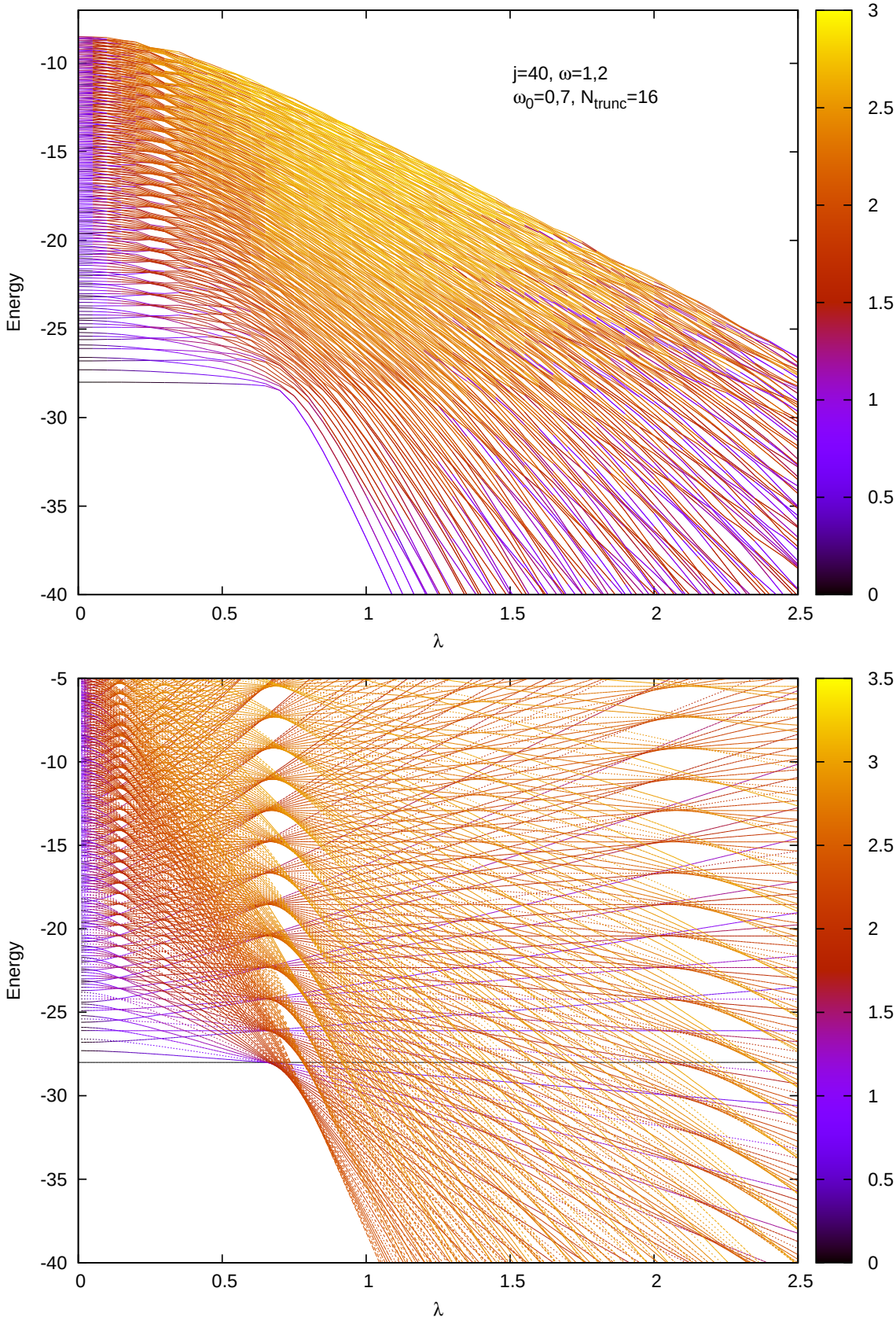

Figure 3.10: Comparison of the Dicke model with its RWA form with the same initial parameters, entropy expressed via colour palette.

Conclusion

Here is a brief summary of what has been achieved:

- We have analyzed QPTs and ESQPTs in the Lipkin model, see Sec. 1.4. In particular, we have associated the critical phenomena with stationary and quasistationary points of the classical potential. The spectra obtained by a numerical diagonalization of the Lipkin Hamiltonian have been shown to be consistent with the classical analysis.

- We have performed a numerical diagonalization of the Dicke and Jaynes-Cummings models, see Sec. 3.1 and 3.2. In the Dicke model, the problem of truncation of the relevant Hilbert space had to be addressed. The spectra of both models have been compared with the results of the classical analysis performed elsewhere, showing the link of of spectral singularities to the features of the respective classical potential.

- We have analyzed the entanglement in the ground and excited states of the Dicke and Jaynes-Cummings models, see Sec. 3.1 and 3.2 and also 2.3. For the Jaynes-Cummings model, the entanglement entropy has been shown to exhibit a singularity close to the ESQPT borderline. The nature of this effect will be a subject of future investigation. No similar critical behaviour of the entanglement has been observed in the non-integrable Dicke model, although in this case the ESQPT seems to be a part of an envelope of the region with maximal entanglement. We have shown that the Dicke and Jaynes-Cummings models yield different predictions of entanglement except a small region in the $\lambda \times E$ region close to $\lambda \simeq 0$.

A. No-Crossing Theorem

Real crossings. To show the 'exceptionality' of real crossings, let us assume that we found one at point λ_0. Energy of a particular level is a solution of the characteristic polynomial

$$\mathfrak{p}\,(\lambda, E) = \det[\hat{H}\,(\lambda) - E \cdot \mathbb{I}]. \tag{A.1}$$

For a real crossing of nth and mth level in λ_0 we get the condition $E_n(\lambda_0) = E_m(\lambda_0) \equiv E_0$. So E_0 is a double root of (A.1), therefore

$$\frac{\partial \mathfrak{p}}{\partial E}\,(\lambda, E)\,|_{E=E_0}^{\lambda=\lambda_0} = 0. \tag{A.2}$$

For fixed E_0 if we slightly vary parameter $\lambda_0 \longrightarrow \lambda_0 \pm \epsilon$ we must get two different roots $E_1 \neq E_2$ for '$+\epsilon$' case and for '$-\epsilon$'case as well. It results in another condition

$$\frac{\partial \mathfrak{p}}{\partial \lambda}\,(\lambda, E)\,|_{E=E_0}^{\lambda=\lambda_0} = 0. \tag{A.3}$$

Two independent formulas (A.2) and (A.3) must be satisfied by varying one parameter which is generally very difficult and can occur only very rarely[1].

[1]To enforce real crossing of two levels, one needs at least two parameters to vary.

B. Singular value decomposition theorem (SVD) and Schmidt decomposition

Theorem 1 (Singular value decomposition)**.** *Suppose Λ is an $m \times n$ real or complex matrix. There exist unitary $m \times m$ and $n \times n$ matrices U and V respectively, such that*

$$U^{+}\Lambda V = \Sigma \tag{B.1}$$

where Σ represents a rectangular diagonal matrix (apparently $m \times n$) of non-negative real numbers known as singular values of Λ.

Proof. $\Lambda^{+}\Lambda$ is obviously a Hermitian matrix. One can easily show that $\Lambda^{+}\Lambda$ is also positive-semidefinite right from the definition: $\langle\xi|\Lambda^{+}\Lambda|\xi\rangle = \|\Lambda|\xi\rangle\|^2 \geq 0$ for an arbitrary vector $|\xi\rangle$. So the spectrum of such a matrix can be written in the descending order as

$$\sigma(\Lambda^{+}\Lambda) = \{\lambda_1, \lambda_2 \ldots \lambda_r, \lambda_{r+1} \ldots \lambda_n\}, \;\; \lambda_1 \geq \lambda_2 \ldots \geq \lambda_r > \lambda_{r+1} \ldots \lambda_n = 0.$$

Here we assume that $n - r$ of the eigenvalues are zeros. One can also form a unitary $n \times n$ matrix V consisting of the eigenvectors $|v_i\rangle$ corresponding to the the eigenvalues λ_i

$$V = [|v_1\rangle, |v_2\rangle \ldots |v_n\rangle].$$

These eigenvectors form a basis in the n-dimensional *column* space. We can use them to form a basis in the m-dimensional *row* space as well. Consider a set of vectors given as

$$|u_i\rangle = \frac{\Lambda|v_i\rangle}{\sqrt{\lambda_i}} \quad \text{for} \;\; i = 1 \ldots r. \tag{B.2}$$

Such vectors are orthogonal

$$\langle u_i|u_j\rangle = \frac{\langle v_i|\Lambda^{+}\Lambda|v_j\rangle}{\sqrt{\lambda_i\lambda_j}} = \lambda_j \frac{1}{\sqrt{\lambda_i\lambda_j}}\delta_{ij} = \delta_{ij}.$$

One can now take this set of vectors $|u_i\rangle$ and extend it to the orthonormal basis

$$[|u_1\rangle, |u_2\rangle \ldots |u_r\rangle \ldots |u_m\rangle]$$

forming the matrix U. Now we can directly show $U^{+}AV = \Lambda$

$$U^{+}\Lambda V = U^{+}\Lambda\left[|v_1\rangle, |v_2\rangle \ldots |v_n\rangle\right] = U^{+}\left[\Lambda|v_1\rangle, \Lambda|v_2\rangle \ldots \Lambda|v_n\rangle\right] =$$

$$= U^{+}\left[\sqrt{\lambda_1}|u_1\rangle, \sqrt{\lambda_2}|u_2\rangle \ldots \sqrt{\lambda_r}|u_r\rangle, |\vec{0}\rangle \ldots |\vec{0}\rangle\right] =$$

$$= \left[\sqrt{\lambda_1}|e_1\rangle, \sqrt{\lambda_2}|e_2\rangle \ldots \sqrt{\lambda_r}|e_r\rangle, |\vec{0}\rangle \ldots |\vec{0}\rangle\right] = \Sigma$$

where we denoted zero vector as $|\vec{0}\rangle$ and the vectors of canonical basis as $|e_i\rangle$ for $i = 1, 2 \ldots$. □

Theorem 2 (Schmidt decomposition)**.** *Suppose $|\Psi\rangle$ is a pure state of a composite system $\mathcal{H} = \mathcal{H}_{\rm l} \otimes \mathcal{H}_{\rm r}$ with dimensions $m = \dim\mathcal{H}_{\rm l}$ and $n = \dim\mathcal{H}_{\rm r}$. Then there exist two sets of orthonormal states $\{|\chi_{{\rm l}i}\rangle\}$ and $\{|\chi_{{\rm r}i}\rangle\}$ such that*

$$|\Psi\rangle = \sum_{i=1}^{\min(m,n)} \sqrt{\rho_i}|\chi_{{\rm l}i}\rangle|\chi_{{\rm r}i}\rangle \tag{B.3}$$

where ρ_i are common eigenvalues of $\hat{\rho}_{\rm r}$ and $\hat{\rho}_{\rm l}$ defined in (2.2) and (2.3).

Proof. To prove this theorem we use (SVD). We denote $\Gamma = \gamma_{ij}$ the matrix of coefficients from eq. (2.1) which is an $m \times n$ matrix associated with Λ from SVD theorem. Therefore $\Gamma = U\Sigma V^+$, where Σ is diagonal with non-negative elements $\Sigma_{kl} = \delta_{kl}\sqrt{\lambda_k}$. Index k counts the number of diagonal terms of a rectangular diagonal matrix therefore its maximum is $k = \min(m, n)$. Then using (2.1) as a starting point one can write

$$|\Psi\rangle = \sum_{ij}(U\Sigma V^+)_{ij}|\psi_{{\rm l}i}\rangle|\psi_{{\rm r}j}\rangle = \sum_{ij}\sum_{k}\left(\sqrt{\lambda_k}U_{ik}(V^+)_{kj}\right)|\psi_{{\rm l}i}\rangle|\psi_{{\rm r}j}\rangle =$$

$$= \sum_k \sqrt{\lambda_k}\underbrace{\sum_i U_{ik}|\psi_{{\rm l}i}\rangle}_{\equiv|\chi_{{\rm l}k}\rangle}\underbrace{\sum_j (V^+)_{kj}|\psi_{{\rm r}j}\rangle}_{\equiv|\chi_{{\rm r}k}\rangle} = \sum_k \sqrt{\lambda_k}|\chi_{{\rm l}k}\rangle|\chi_{{\rm r}k}\rangle.$$

Unitary operators U and V^+ transform basis vectors $|\psi_{{\rm l}i}\rangle$ and $|\psi_{{\rm r}j}\rangle$ to new sets of orthonormal bases $\{|\chi_{{\rm l}i}\rangle\}_{i=1}^m, \{|\chi_{{\rm r}j}\rangle\}_{j=1}^n$. According to SVD the coefficients λ_k are eigenvalues of $\Gamma^+\Gamma$ which is in our case $\Gamma^+\Gamma = \rho_{{\rm r}jj'}$. Its diagonalization $\rho_{{\rm r}jj'} = \delta_{jj'}\rho_j$ leads to the diagonalization of $\hat{\rho}_{\rm r} = \sum_j \rho_j|\psi_{{\rm r}j}\rangle\langle\psi_{{\rm r}j}|$. Therefore the coefficients λ_k are equal to the eigenvalues ρ_j of $\hat{\rho}_{\rm r}$. Now the only thing which is left to be proved is whether the coefficients ρ_j are also eigenvalues of $\hat{\rho}_{\rm r}$. This can be seen as follows

$$\hat{\rho}_{\rm l} = {\rm Tr}_{\rm r}\left[\sum_{ij}\sqrt{\rho_i}\sqrt{\rho_j}|\chi_{{\rm l}i}\rangle|\chi_{{\rm r}i}\rangle\langle\chi_{{\rm l}j}|\langle\chi_{{\rm r}j}|\right] =$$

$$= \sum_k \langle\chi_{{\rm r}k}|\left[\sum_{ij}\sqrt{\rho_i}\sqrt{\rho_j}|\chi_{{\rm l}i}\rangle|\chi_{{\rm r}i}\rangle\langle\chi_{{\rm l}j}|\langle\chi_{{\rm r}j}|\right]|\chi_{{\rm r}k}\rangle = \sum_i \rho_i|\chi_{{\rm l}i}\rangle\langle\chi_{{\rm l}j}|$$

where we used orthonormality

$$\langle\chi_{{\rm r}k}|\chi_{{\rm r}i}\rangle = \sum_{ll'} V_{lk}V^+_{il'}\underbrace{\langle\psi_{{\rm r}l}|\psi_{{\rm r}l'}\rangle}_{\delta_{ll'}} = \sum_l V_{lk}V^+_{il} = \delta_{ik}.$$

The last equality holds because V is unitary.

Obviously in case of dimensional mismatch $m \neq n$, say $m > n$, $\rho_i = 0$ for $i > n$ in the larger space. □

C. Schwinger mapping and Holstein-Primakoff transformation

Schwinger representation. For $U(2)$ symmetry-based models, such as two-dimensional harmonic oscillator, the generators of the symmetry algebra can be formed as bilinear products of creation and annihilation operators $\hat{s}^+\hat{s},\ \hat{s}^+\hat{t},\ \hat{t}^+\hat{s},\ \hat{t}^+\hat{t}$. However these generators can be rearranged to physically meaningful operators

$$\begin{aligned} \hat{J}_x &= \frac{1}{2}\left(\hat{t}^+\hat{s} + \hat{s}^+\hat{t}\right),\ \hat{J}_y = \frac{i}{2}\left(\hat{s}^+\hat{t} - \hat{t}^+\hat{s}\right), \\ \hat{J}_z &= \frac{1}{2}\left(\hat{t}^+\hat{t} - \hat{s}^+\hat{s}\right),\ \hat{N} = \hat{s}^+\hat{s} + \hat{t}^+\hat{t}, \end{aligned} \tag{C.1}$$

where $\hat{N}$ is the operator of the total number of s and t bosons[1]. Knowing the commutation relation of the single bosonic s and t operators one can show that the commutation relation $[\hat{J}_i, \hat{J}_j] = i\varepsilon_{ijk}\hat{J}_k$ is satisfied for $\{ijk\} \leftrightarrow \{xyz\}$ and therefore these operators can be referred to as projection operators of the total angular momentum.

From the quantum theory of angular momentum we know how to construct the *ladder* operators $\hat{J}_\pm = \hat{J}_x \pm i\hat{J}_y$ so

$$\hat{J}_+ = \hat{t}^+\hat{s},\ \ \hat{J}_- = \hat{s}^+\hat{t}. \tag{C.2}$$

Since $\hat{N}$ is conserved by (C.1) the subspace with a given value of N (with dimension $d = N+1$) carries an irreducible representation of the angular momentum algebra with $j = \frac{N}{2}$.

Holstein-Primakoff transformation. This transformation represents *one-to-one* correspondence between the angular momentum operators and boson creation and annihilation operators, here denoted as $\hat{b}^+$ and $\hat{b}$. The lowest weight state $|j - j\rangle$ can be associate with the b-boson vacuum $|0\rangle$. Then for any integer $n \leq 2j$ we can also associate

$$|j(-j+n)\rangle \leftrightarrow \frac{\left(\hat{b}^+\right)^n}{\sqrt{n!}}|0\rangle. \tag{C.3}$$

Now, lets see how the ladder operators transform

[1] Or equivalently $\hat{N}$ is the operator which counts the total number of phonons in the two-dimensional oscillator.

$$
\begin{aligned}
&\hat{J}_+|j(-j+n)\rangle = \sqrt{j\,(j+1)-(-j+n)\,(-j+n+1)}|j(-j+n+1)\rangle \\
&= \sqrt{2j\,(n+1)+n\,(n+1)}|j(-j+n+1)\rangle \\
&= \sqrt{n+1}\sqrt{2j+n}|j(-j+n+1)\rangle = \sqrt{n+1}\sqrt{2j+n}\frac{\left(\hat{b}^+\right)^{n+1}}{\sqrt{(n+1)!}}|0\rangle \\
&= \sqrt{2j+n}\hat{b}^+\frac{\left(\hat{b}^+\right)^{n}}{\sqrt{n!}}|0\rangle = \hat{b}^+\sqrt{2j+n}|j(-j+n)\rangle \\
&= \hat{b}^+\sqrt{2j+\hat{b}^+\hat{b}}|j(-j+n)\rangle
\end{aligned}
\tag{C.4}
$$

where in the last step we associated n with the total number of b bosons. Its maximal value $N_b^{\max}$ must be equal to $2j$.

Similarly for the lowering ladder operator

$$
\begin{aligned}
&\hat{J}_-|j(-j+n)\rangle = \sqrt{j\,(j+1)-(n-j)\,(-j+n-1)}|j(-j+n-1)\rangle \\
&= \sqrt{2j-(n-1)}\sqrt{n}|j(-j+n-1)\rangle = \sqrt{2j-(n-1)}\sqrt{n}\frac{\left(\hat{b}^+\right)^{n-1}}{\sqrt{(n-1)!}}|0\rangle \\
&= \sqrt{2j-(n-1)}\;\hat{b}\frac{\left(\hat{b}^+\right)^{n}}{\sqrt{!}}|0\rangle = \sqrt{2j-\hat{b}^+\hat{b}}\;\hat{b}\frac{\left(\hat{b}^+\right)^{n}}{\sqrt{n!}}|0\rangle \\
&= \sqrt{2j-\hat{b}^+\hat{b}}\;\hat{b}|j(-j+n)\rangle.
\end{aligned}
\tag{C.5}
$$

The transformation of $\hat{J}_0$ is straightforward

$$
\begin{aligned}
&\hat{J}_0|j(-j+n)\rangle = (n-j)|j(-j+n)\rangle = (n-j)\frac{\left(\hat{b}^+\right)^{n}}{\sqrt{n!}}|0\rangle \\
&= \left(\hat{b}^+\hat{b}-j\right)|j(-j+n)\rangle.
\end{aligned}
\tag{C.6}
$$

One can notice that the Holstein-Primakoff mapping can be formally obtained from Schwinger mapping via substitution $\hat{t},\hat{t}^+ \mapsto \hat{b},\hat{b}^+$ and $\hat{s},\hat{s}^+ \mapsto \sqrt{2j-\hat{b}^+\hat{b}}$.

D. Numerical solution of the Dicke Hamiltonian

Truncation. As noted in Section 3.1 truncation of the total number of photons is needed in numerical study of the Dicke model. So we have a system of N_{a} spin sites (or two-level atoms equivalently) and a truncated number of photons N_{tr} with a dimension $(N_{\mathrm{a}}+1)(N_{\mathrm{tr}}+1)$. The question is, how well does the spectrum of such a system approximate the Dicke model.

One must keep in mind that individual levels interact with one another. One can anticipate that the top levels in the truncated spectrum will definitely not be a good approximation because of the absence of the levels right above them. However the levels closer to the ground state would be affected only a little by the missing part of the full Dicke spectrum. So we can suppose that the contribution of the absent levels to the 'ground state area' is negligible and this part of the spectrum is a good approximation of the Dicke model.

In our numerical solution we establish N_{tr} from the given number N_{lev} of required relevant levels. We do so by comparing the N_{lev}th level energy in two runs of the program for N_{tr} and $N_{\mathrm{tr}}+1$ considering the maximal interaction in λ_{max}. If the difference is sufficiently small[1] we take the current N_{tr} as a relevant truncation needed to obtain N_{lev} levels of the Dicke model. Here we present the relevant scripts written in GNU Octave.

The script computing the free part of the Hamiltoninan 3.1.

```
function FreeDicke=FreeDicke(Na,w0,Ntr,w)
 % parameters: Na-number of the 2-level atoms,
       % Ntr-truncated number of photons,
 % w0 - 1-particle enery of 2-level atoms,
       % w - 1-particle enery of photons,

j=Na/2;

FreeDicke=zeros((Na+1)*(Ntr+1));
FDJ=zeros((Na+1)*(Ntr+1));
FDGamma=zeros((Na+1)*(Ntr+1));

m=-j;
for ind=1:(Ntr+1):Na*(Ntr+1)+1
    FDJ(ind:ind+Ntr,ind:ind+Ntr)=w0*m*eye(Ntr+1);
    m=m+1;
end

for n=1:(Ntr+1):Na*(Ntr+1)+1
    FDGamma(n:n+Ntr,n:n+Ntr)=w*diag(0:Ntr);
end
```

[1] In our program we set a condition that the energy of the maximal N_{lev}th level must be equal in eight significant digits in both runs. Note that GNU Octave that was used fot numerical study works with the double precision.

```
FreeDicke=FDJ+FDGamma;
```

The script computing the interaction part of the Hamiltoninan 3.1.

```
function InterakceDicke=InterakceDicke(Na,Ntr)
% parameters: Na–number of the 2–level atoms,
      % Ntr–truncated number of photons,
  J=zeros(Na+1,Na+1);
  Gamma=zeros(Ntr+1);
  ONNa=eye(Na+1);   %orthogonal matrix
  ONNtr=eye(Ntr+1);
  j=Na/2;
  InterakceDicke=zeros((Na+1)*(Ntr+1));

 %contribution of (J^{+}+J) in spin states

for m=(-j):(j)
   if (abs(m)<=j-1)
     vecPlusNa=sqrt(j*(j+1)-m*(m+1))*ONNa(:,m+j+1+1);
     vecMinusNa=sqrt(j*(j+1)-m*(m-1))*ONNa(:,m+j+1-1);
   elseif (m==j)
     vecPlusNa=0;
     vecMinusNa=sqrt(j*(j+1)-m*(m-1))*ONNa(:,m+j+1-1);
   else
    vecPlusNa=sqrt(j*(j+1)-m*(m+1))*ONNa(:,m+j+1+1);
     vecMinusNa=0;
   end
   J(:,m+j+1)= vecPlusNa+ vecMinusNa;
 end


  %contribution of (b^{+}+b) in photon states
 for n=(0):(Ntr)
    if (n==0)
     vecPlusNtr= sqrt(n+1)*ONNtr(:,n+1+1);
     vecMinusNtr=0;
   elseif  (n==Ntr)
     vecPlusNtr= 0;
     vecMinusNtr=sqrt(n)*ONNtr(:,n+1-1);
   else
     vecPlusNtr= sqrt(n+1)*ONNtr(:,n+1+1);
     vecMinusNtr=sqrt(n)*ONNtr(:,n+1-1);
   end
   Gamma(:,n+1)=vecPlusNtr+vecMinusNtr;
 end


  %mind the position in the matrix!!
 for i=1:(Ntr+1):(Na)*(Ntr+1)+1
  for k=1:(Ntr+1):(Na)*(Ntr+1)+1
```

```
      InterakceDicke(i:i+Ntr,k:k+Ntr)=
           J(idivide(i,Ntr+1)+1,idivide(k,Ntr+1)+1).*Gamma;
    end
  end
```

The script computing the Dicke Hamiltonian with λ_{max} 3.1. This function is used in the truncation as noted above.

```
function TruncDicke=TruncDicke(NA,w0,N,w)
 % parameters: Na–number of 2level atoms,
 % N–number of photons  in the run
 % w0 – 1–particle enery of 2–level atoms,
       % w – 1–particle enery of photons,
 % for max lambda=3

j=NA/2;
TruncDicke=FreeDicke(NA,w0,N,w)+3/(4*j)*InterakceDicke(NA,N);
```

Diagonalization of the Dicke Hamiltonian 3.1.

```
%Dicke model
 NA=input('Number of spin sites: ');
 Nlev=input('Number of required levels: ');

 %Ntr=40;
  w0=1;
  w=1;

  %Truncation
  N=idivide(Nlev,NA+1)+1;

  while (1)
   Ini=zeros((NA+1)*(N+1));
   Next=zeros((NA+1)*(N+2));
   Ini=TruncDicke(NA,w0,N,w);
   Next=TruncDicke(NA,w0,N+1,w);
   EigNext=eig(Next);
   EigIni=eig(Ini);

   if (str2num(num2str(EigNext(Nlev),8))
        ==str2num(num2str(EigIni(Nlev),8)))
    break;
   else
      N=N+1;
   end
  end
 Ntr=N;



 j=NA/2;
```

```
data=zeros(61,(NA+1)*(Ntr+1)+1);%dimension must fit for-cycle

ind=1;
 for lambda=0.0:0.05:3.0
   DickeHam=FreeDicke(NA,w0,Ntr,w)
    +lambda/sqrt((4*j))*InterakceDicke(NA,Ntr);
  v = eig(DickeHam);
  vektor = [lambda v' ];
  data(ind,:)=vektor;
  ind=ind+1;
 end

    save -ascii "Dicke.dat" data ;
```

E. Rotating wave approximation (RWA)

Brief overview. This approximation is used in atomic physics and its basic idea is that the terms in Hamiltonian which oscillate rapidly are averaged to zero and therefore can be neglected.

In the first step we move into the interaction picture of the Dicke Hamiltonian $\hat{H}_{\mathrm{D}} \to \hat{H}_{\mathrm{D}}^{\mathrm{int}}$. The time dependence for the operator $\hat{b}$ is then given as

$$\frac{\mathrm{d}\hat{b}}{\mathrm{d}t} = i[\hat{H}_{\mathrm{free}}, \hat{b}] = i\omega[\hat{b}^{+}\hat{b}, \hat{b}] = -i\omega\hat{b} \Rightarrow \hat{b}(t) = \hat{b}(0)\mathrm{e}^{-i\omega t}. \tag{E.1}$$

Similarly in the interaction picture one can show

$$\hat{b}^{+}(t) = \hat{b}^{+}(0)\mathrm{e}^{i\omega t}, \;\; \hat{J}_{-}(t) = \hat{J}_{-}(0)\mathrm{e}^{-i\omega_0 t}, \;\; \hat{J}_{+}(t) = \hat{J}_{+}(0)\mathrm{e}^{i\omega_0 t}. \tag{E.2}$$

So one can easily see that the terms $\hat{b}^{+}\hat{J}_{+}$ are $\hat{b}^{-}\hat{J}_{-}$ (so called *counter-rotating terms*) oscillate with frequency $\omega_0 + \omega$ which is faster than in the case of $\hat{b}^{+}\hat{J}_{-}$ and $\hat{b}\hat{J}_{+}$. When the one-particle energies get close to resonance, the diference in the final frequencies becomes more significant. At this point one usually omits the counter-rotating terms as they average to zero over the reasonable time period. Now we move back to the Schrödinger picture and obtain the Jaynes-Cummings Hamiltonian $\hat{H}_{\mathrm{JC}}$.

Bibliography

[1] HERTZ J., Phys. Rev. B 14 **3** (1976) 1165–1184.

[2] GILMORE R., FENG D. H., Nucl. Phys. A **301** (1978) 189.

[3] CAPRIO M. A., CEJNAR P., IACHELLO F., Ann. Phys. **323** (2008) 1106-1135.

[4] CEJNAR P., STRÁNSKÝ P., Phys. Rev. E **78** (2008) 031130.

[5] OSTERLOH A., AMICO L., FALCI G., FAZIO R., Nature **416** (2002) 608.

[6] PECHUKAS P., Phys. Rev. Lett. **51** (1983) 943-946.

[7] YUKAWA T., Phys. Rev. Lett. **54** (1985) 1883-1886.

[8] CEJNAR P. JOLIE J., Prog. Part. Nucl. Phys. **62** (2009) 210

[9] MORÁVEK P., Bachelor thesis, 2008

[10] SACHDEV S., *Quantum Phase Transitions*, Cambridge University Press. (2nd ed.), ISBN 978-0-521-51468-2.

[11] CARR L. D., *Understanding Quantum Phase Transitions*, CRC Press 2010, ISBN 978-1-4398-0251-9.

[12] CEJNAR P., Journal of Phys.: Conference Series **322** (2011) 012012.

[13] PÉREZ-FERNÁNDEZ P., CEJNAR P., ARIAS J. M., DUKELSKY J., GARCÍA-RAMOS J. E., RELANO A., Phys. Rev. A **83** (2011) 033802.

[14] LIPKIN H. J., MESHKOV N., GLICK A. J., Nuclear Phys.**62** (1965) 188.

[15] FRANK A., VAN ISACKER P., *Symmetry Methods in Molecules and Nuclei*, (2nd ed.), SyG, Mexico (2005).

[16] HOLSTEIN T., PRIMAKOFF H. Phys. Rev. **58** (1940) 1098 - 1113.

[17] PÉREZ-FERNÁNDEZ P., RELANO A., ARIAS J. M., DUKELSKY J., GARCÍA-RAMOS J. E., Phys. Rev. A **80** (2009) 032111.

[18] EINSTEIN, A., PODOLSKY, B., ROSEN, N., Phys. Rev. **47** (1935) 777–780.

[19] CEJNAR P., *A Condensed Course of Quantum Mechanics*, Karolinum 2013 to be published .

[20] WOOTTERS W. K., Phys. Rev. Lett. **80** (1997) 2245 .

[21] PLENIO M. B., VIRMANI S., Quant. Inf. Comp, **7** (2007) 001-051.

[22] LAMBERT N., EMARY C., BRANDES T., Phys. Rev. Lett. **92** (2004) 073602.

[23] DICKE R. H., Phys. Rev. **93** (1954) 99.

[24] EMARY C., BRANDES T., Phys. Rev. E **67** (2003) 066203.

[25] FRASCO M. Ann.Phys. **306** (2003) 193-208.

List of Abbreviations

QPT - Quantum phase transition
ESQPT - Excited-state quantum phase transition
SVD - Singular value decomposition
RWA - Rotating wave approximation